

Contents

| | page |
|---|------|
| Velocity of Sound in Liquid Propane. Ben A. Younglove | 165 |
| Models of Quasi-Steady and Unsteady Discharge from Plumbing Fixtures. Bal M. Mahajan, Lawrence S. Galwin, and Paul A. Kopetka | 171 |
| Transition Temperatures of the Hydrates of Na_2SO_4 , Na_2HPO_4 , and KF as Fixed Points in Biomedical Thermometry. R. L. Magin, B. W. Mangum, J. A. Statler, and D. D. Thornton . | 181 |
| A Game-Theoretic Model of Inspection-Resource Allocation. Martin H. Pearl and Alan J. Goldman | 193 |
| Publications of the National Bureau of Standards | 217 |

Library of Congress Catalog Card Number: 63-37059

For sale by the Superintendent of Documents, U.S. Government Printing Office.
Washington, D.C. 20402. Order by SD Catalog
No. C13.22/vol. 86(2). Single copy price \$3 Domestic; \$3.75 Foreign.
Subscription price: \$13 a year; \$4.25 additional for foreign mailing.

UNITED STATES GOVERNMENT PRINTING OFFICE, WASHINGTON: 1981

Velocity of Sound in Liquid Propane*

Ben A. Younglove†

National Bureau of Standards, Boulder, CO 80303

November 19, 1980

Sound velocity measurements on liquid propane from 90 to 300 K and for pressures to 34 MPa are reported. Also included are saturated liquid sound velocities from 90 to 290 K. The data were combined with $P\rho T$ data to compute compressibility and specific heat ratio. Comparisons were made to computed values of sound velocity of Goodwin and to the data of Lacam.

Key words: Adiabatic compressibility; liquid; pressure; propane; sound; specific heat ratios; speed; temperature; velocity.

1. Introduction

Thermodynamic and transport properties of propane are valuable to the energy industry in the design calculations relating to the handling, transporting, and storage of liquefied natural gas. The data of this paper were obtained as part of a program to provide accurate thermodynamic properties data for propane to support the energy industry, especially the liquefied natural gas industry.

Measurements of sound velocity were made from 90 K to 290 K in the saturated liquid and from 90 K to 300 K and at pressures to 34 MPa in the compressed liquid.

Sound velocities, W , were related to the adiabatic compressibility, k , using

$$W = (\rho k_s)^{-1/2} \quad (1)$$

and to the specific heat ratio, γ , using

$$W = (\gamma \frac{\partial P}{\partial \rho})_T^{1/2}, \quad (2)$$

where P , ρ and T are pressure, density, and temperature respectively.

2. Experimental Procedure

Sound velocities were measured using a pulse superposition method. Pulses were generated with a 10 MHz quartz crystal and were allowed to reflect between a matched crystal mounted plane and parallel to the generating

crystal. Pulses were generated at a rate such that the reflected pulses were superposed with the new pulses. This condition is detected with an oscilloscope by maximizing the resulting reinforced waveshape as seen by the receiving crystal. This technique, developed by Greenspan and Tschiegg [1],¹ has been used on hydrogen [2], oxygen [3], fluorine [4], methane [5], and ethane [6] in this laboratory and the apparatus is described in detail in the earlier publications. Uncertainty in the measured sound velocities is estimated to be 0.05 percent. Temperatures were measured using a platinum resistance thermometer calibrated by the National Bureau of Standards on the IPTS 1968. Uncertainty in temperature is estimated to be 0.005 K at the lower temperatures and increasing to 0.03 K at 300 K⁶.

The sample propane was commercially available ultra high purity grade (99.97 mole percent propane).

3. Results

Experimental values of sound velocity and temperature for the saturated liquid are given in table I with the corresponding values of density, compressibility, and specific heat ratio. Table II gives the same quantities for the compressed liquid with the measured values of pressure on isotherms. Isotherms were at 10 K increments from 90 to 120 K and at 20 K increments from 120 to 300 K, and for pressures to 34 MPa. Densities, corresponding to the measured values of temperature and pressure were computed from the recent $P\rho T$ surface of Goodwin [7,8]. These data are shown in figure 1.

Experimental uncertainty in compressibility of 0.3 percent is a result of the combined uncertainties in density and

*This work was carried out at the National Bureau of Standards under the sponsorship of the Gas Research Institute.

†Thermophysical Properties Division, National Engineering Laboratory.

¹ Figures in brackets indicate literature references at the end of this paper.

sound velocity. The corresponding uncertainty for the specific heat ratio, γ , is 4 percent which is due to the uncertainty in the derivative $(\frac{\partial P}{\partial \rho})_T$. Ethane has very low compressibility in the liquid phase, certainly so when compared with methane [5] and even with ethane [6]. The very rapid increase in pressure with respect to density puts considerable demands on the ability of the $P_Q T$ surface to produce this derivative accurately since a small uncertainty in density corresponds to a very much larger uncertainty in pressure. The uncertainty in the density measurements on which the $P_Q T$ is based will reflect in a much larger uncertainty in a calculated pressure and even more uncertainty in a calculated value of the derivative $(\frac{\partial P}{\partial \rho})_T$.

Lacam [9] has measured sound velocities at 298.15 K (25 °C) and at 25 K increments to 498.15 K (225 °C) for pressures to 101 MPa. Figure 2 shows a comparison of his 25 C isotherm to the 280 K and 300 K isotherms of this report, where Goodwin's [8] computed sound velocities were used to make the comparison. It can be seen that there is about 0.2 to 0.3 percent difference in the two sets of measurements, which is within the combined uncertainties of the measurements Lacam estimated his uncertainties at 0.3 percent in sound velocity exclusive of temperature and pressure uncertainty contributions.

4. References

- [1] Greenspan, M.; Tschiegg, C.E. Speed of sound in water by a direct method. *59*(4): 249-254; 1957 October.
- [2] Younglove, B. A. Speed of sound in fluid parahydrogen. *J. Acoust. Soc. Am.* **38**: 433-438; (1965).
- [3] Straty, G. C.; Younglove, B. A. Velocity of sound in saturated and compressed fluid oxygen. *J. Chem. Thermo.* **5**: 305-312; (1973).
- [4] Straty, G. C.; Younglove, B. A. Some sound velocity measurements on liquid fluorine. *J. Chem. Phys.* **58**: 2191-2192; (1973).

- [5] Straty, G. C. Velocity of sound in dense fluid methane. *Cryogenics.* **14**: 367-370; (1974).
- [6] Tsumura, R.; Straty, G. C. Speed of sound in saturated and compressed fluid ethane. *Cryogenics.* **17**: 195-200; (1977).
- [7] Goodwin, R. D. The nonanalytic equation of state for pure fluids applied to propane. *Advances in Chemistry Series No. 182*, The American Chemical Society, Publishers, pp. 345-64. (176th National Meeting of the American Chemical Society, Miami Beach, Florida, Sept. 10-15, 1978.)
- [8] Goodwin, R. D. Provisional thermodynamic functions of propane, from 85 to 700 K at Pressures to 700 Bar, *Nat. Bur. Stand. (U.S.)*, Interagency Report NBSIR 77-860.
- [9] Lacam, A. Etude experimentale de la propagation des ultrasons dans les fluides. *J. Recherches C.N.R.S.* **34**: 25-56; (1956).

TABLE I. Experimental values of saturated liquid sound velocity, W_E , and temperature, T , with values of sound velocity, W_c , and density, ρ , computed from the $P_Q T$ surface [ref. 7, 8]. The adiabatic compressibility, K_s , and heat capacity ratio, γ , were computed from W_E and $P_Q T$ derived properties.

| T K | W_E m/s | W_c m/s | Δ % | ρ mol/L | K_s GPa ⁻¹ | γ |
|----------|--------------|--------------|---------------|-----------------|----------------------------|----------|
| 90.0 | 2106.2 | 2115.8 | 0.46 | 16.52 | 0.309 | 1.366 |
| 100.0 | 2037.6 | 2020.8 | -0.82 | 16.29 | .335 | 1.418 |
| 110.0 | 1969.2 | 1932.5 | -1.86 | 16.06 | .364 | 1.462 |
| 120.0 | 1900.8 | 1849.7 | -2.69 | 15.83 | .396 | 1.500 |
| 130.0 | 1832.6 | 1771.3 | -3.34 | 15.61 | .433 | 1.531 |
| 140.0 | 1764.9 | 1696.6 | -3.87 | 15.37 | .474 | 1.557 |
| 150.0 | 1697.4 | 1625.1 | -4.26 | 15.14 | .520 | 1.578 |
| 160.0 | 1630.3 | 1556.1 | -4.55 | 14.91 | .572 | 1.594 |
| 170.0 | 1563.3 | 1489.3 | -4.74 | 14.68 | .632 | 1.606 |
| 180.0 | 1496.5 | 1424.3 | -4.82 | 14.44 | .701 | 1.615 |
| 190.0 | 1430.0 | 1360.9 | -4.83 | 14.20 | .781 | 1.620 |
| 200.0 | 1364.4 | 1298.7 | -4.81 | 13.95 | .873 | 1.625 |
| 210.0 | 1298.5 | 1237.6 | -4.69 | 13.71 | .981 | 1.626 |
| 230.0 | 1167.1 | 1117.6 | -4.25 | 13.20 | 1.261 | 1.623 |
| 250.0 | 1036.5 | 999.3 | -3.59 | 12.66 | 1.667 | 1.618 |
| 260.0 | 971.6 | 940.4 | -3.20 | 12.37 | 1.941 | 1.617 |
| 270.0 | 905.4 | 881.5 | -2.65 | 12.08 | 2.290 | 1.614 |
| 290.0 | 775.1 | 762.2 | -1.67 | 11.44 | 3.298 | 1.624 |

TABLE II. Experimental values of compressed liquid sound velocity, W_E , temperature T , and pressure, P . Sound velocity, W_c , and density, ρ , were computed from the P ρ T surface (ref. 7,8). Adiabatic compressibility, K_s , and specific heat ratio were computed from W_E and properties derived from the P ρ T surface.

| W_E m/s | W_c m/s | Δ % | P MPa | T K | ρ mol/L | K_s GPa ⁻¹ | γ |
|--------------|--------------|---------------|------------|----------|-----------------|----------------------------|----------|
| 2205.44 | 2337.55 | 5.99 | 34.83 | 90.00 | 16.739 | 0.279 | 1.218 |
| 2196.20 | 2316.63 | 5.48 | 31.43 | 90.00 | 16.719 | .281 | 1.231 |
| 2190.77 | 2304.92 | 5.21 | 29.54 | 90.00 | 16.708 | .283 | 1.237 |
| 2188.78 | 2299.81 | 5.07 | 28.71 | 90.00 | 16.703 | .283 | 1.241 |
| 2179.03 | 2277.51 | 4.52 | 25.13 | 90.00 | 16.682 | .286 | 1.254 |
| 2173.65 | 2266.16 | 4.26 | 23.32 | 90.00 | 16.671 | .288 | 1.261 |
| 2156.54 | 2227.63 | 3.30 | 17.22 | 90.00 | 16.633 | .293 | 1.286 |
| 2149.02 | 2210.83 | 2.88 | 14.58 | 90.00 | 16.616 | .296 | 1.298 |
| 2138.05 | 2190.05 | 2.45 | 11.42 | 90.00 | 16.595 | .299 | 1.310 |
| 2132.21 | 2173.98 | 1.96 | 8.86 | 90.00 | 16.578 | .301 | 1.324 |
| 2123.73 | 2155.66 | 1.50 | 6.05 | 90.00 | 16.559 | .304 | 1.336 |
| 2114.18 | 2134.37 | .95 | 2.80 | 90.00 | 16.537 | .307 | 1.352 |
| 2143.33 | 2239.98 | 4.51 | 34.57 | 100.00 | 16.533 | .299 | 1.266 |
| 2130.73 | 2212.04 | 3.82 | 29.99 | 100.00 | 16.504 | .303 | 1.284 |
| 2120.78 | 2191.23 | 3.32 | 26.61 | 100.00 | 16.482 | .306 | 1.297 |
| 2111.08 | 2170.90 | 2.83 | 23.34 | 100.00 | 16.460 | .309 | 1.310 |
| 2101.98 | 2151.91 | 2.38 | 20.31 | 100.00 | 16.439 | .312 | 1.324 |
| 2092.18 | 2131.84 | 1.90 | 17.12 | 100.00 | 16.417 | .316 | 1.337 |
| 2083.40 | 2113.72 | 1.46 | 14.27 | 100.00 | 16.397 | .319 | 1.349 |
| 2075.42 | 2097.28 | 1.05 | 11.70 | 100.00 | 16.379 | .321 | 1.361 |
| 2065.52 | 2077.08 | .56 | 8.57 | 100.00 | 16.356 | .325 | 1.375 |
| 2056.28 | 2058.59 | .11 | 5.73 | 100.00 | 16.334 | .328 | 1.390 |
| 2046.52 | 2040.08 | -.31 | 2.91 | 100.00 | 16.313 | .332 | 1.402 |
| 2082.37 | 2151.94 | 3.34 | 34.56 | 110.00 | 16.330 | .320 | 1.305 |
| 2073.64 | 2134.77 | 2.95 | 31.73 | 110.00 | 16.310 | .323 | 1.316 |
| 2064.95 | 2117.48 | 2.54 | 28.90 | 110.00 | 16.290 | .326 | 1.327 |
| 2056.27 | 2100.33 | 2.14 | 26.12 | 110.00 | 16.270 | .330 | 1.339 |
| 2053.58 | 2094.18 | 1.98 | 25.12 | 110.00 | 16.262 | .331 | 1.344 |
| 2049.41 | 2086.45 | 1.81 | 23.88 | 110.00 | 16.253 | .332 | 1.349 |
| 2038.65 | 2065.26 | 1.31 | 20.49 | 110.00 | 16.228 | .336 | 1.363 |
| 2028.89 | 2046.46 | .87 | 17.51 | 110.00 | 16.205 | .340 | 1.377 |
| 2018.84 | 2027.12 | .41 | 14.46 | 110.00 | 16.182 | .344 | 1.390 |
| 2009.49 | 2009.27 | -.01 | 11.68 | 110.00 | 16.160 | .348 | 1.403 |
| 1999.34 | 1989.62 | -.49 | 8.65 | 110.00 | 16.135 | .352 | 1.418 |
| 1989.58 | 1971.14 | -.93 | 5.82 | 110.00 | 16.112 | .356 | 1.432 |
| 1979.93 | 1952.74 | -1.37 | 3.03 | 110.00 | 16.089 | .360 | 1.446 |
| 2022.84 | 2071.43 | 2.40 | 34.73 | 120.00 | 16.128 | .344 | 1.338 |
| 2011.06 | 2048.79 | 1.88 | 31.00 | 120.00 | 16.099 | .348 | 1.354 |
| 2003.04 | 2034.46 | 1.57 | 28.66 | 120.00 | 16.081 | .351 | 1.363 |
| 1989.88 | 2011.17 | 1.07 | 24.90 | 120.00 | 16.051 | .357 | 1.378 |
| 1975.15 | 1983.23 | .41 | 20.44 | 120.00 | 16.015 | .363 | 1.398 |
| 1964.44 | 1963.68 | -.04 | 17.35 | 120.00 | 15.989 | .368 | 1.413 |
| 1953.21 | 1943.44 | -.50 | 14.19 | 120.00 | 15.963 | .372 | 1.426 |
| 1944.42 | 1927.68 | -.86 | 11.76 | 120.00 | 15.941 | .376 | 1.439 |
| 1933.20 | 1907.48 | -1.33 | 8.66 | 120.00 | 15.914 | .381 | 1.454 |
| 1921.82 | 1885.74 | -1.88 | 5.37 | 120.00 | 15.884 | .387 | 1.472 |
| 1912.43 | 1870.40 | -2.20 | 3.07 | 120.00 | 15.863 | .391 | 1.483 |
| 1905.10 | 1924.60 | 1.02 | 34.90 | 140.00 | 15.724 | .397 | 1.389 |
| 1895.45 | 1908.54 | .69 | 32.29 | 140.00 | 15.701 | .402 | 1.399 |
| 1882.90 | 1887.82 | .26 | 28.94 | 140.00 | 15.671 | .408 | 1.413 |
| 1873.05 | 1871.52 | -.08 | 26.34 | 140.00 | 15.647 | .413 | 1.424 |
| 1859.89 | 1849.90 | -.54 | 22.93 | 140.00 | 15.615 | .420 | 1.439 |
| 1850.14 | 1833.37 | -.91 | 20.35 | 140.00 | 15.590 | .425 | 1.451 |
| 1839.27 | 1816.03 | -1.26 | 17.66 | 140.00 | 15.563 | .431 | 1.464 |

TABLE II. *Experimental values of compressed liquid sound velocity, W_E , temperature T , and pressure, P . Sound velocity, W_c , and density, ρ , were computed from the PqT surface (ref. 7,8). Adiabatic compressibility, K , and specific heat ratio were computed from W_E and properties derived from the PqT surface.—Continued.*

| W_E m/s | W_c m/s | Δ % | P MPa | T K | ρ mol/L | K , GPa ⁻¹ | γ |
|--------------|--------------|---------------|------------|----------|-----------------|----------------------------|----------|
| 1825.05 | 1793.00 | -1.76 | 14.15 | 140.00 | 15.528 | .438 | 1.480 |
| 1813.01 | 1773.54 | -2.18 | 11.22 | 140.00 | 15.498 | .445 | 1.495 |
| 1801.58 | 1754.90 | -2.59 | 8.44 | 140.00 | 15.468 | .452 | 1.510 |
| 1790.56 | 1737.34 | -2.97 | 5.86 | 140.00 | 15.441 | .458 | 1.523 |
| 1779.49 | 1719.92 | -3.35 | 3.33 | 140.00 | 15.413 | .465 | 1.537 |
| 1788.31 | 1790.01 | .10 | 34.57 | 160.00 | 15.319 | .463 | 1.422 |
| 1777.79 | 1773.82 | -.22 | 31.99 | 160.00 | 15.292 | .469 | 1.433 |
| 1764.69 | 1753.94 | -.61 | 28.86 | 160.00 | 15.259 | .477 | 1.446 |
| 1753.72 | 1737.38 | -.93 | 26.28 | 160.00 | 15.232 | .484 | 1.457 |
| 1739.54 | 1716.50 | -1.32 | 23.07 | 160.00 | 15.196 | .493 | 1.471 |
| 1726.90 | 1697.22 | -1.72 | 20.15 | 160.00 | 15.163 | .501 | 1.485 |
| 1715.11 | 1679.69 | -2.07 | 17.53 | 160.00 | 15.133 | .509 | 1.497 |
| 1700.99 | 1659.01 | -2.47 | 14.48 | 160.00 | 15.097 | .519 | 1.512 |
| 1673.66 | 1618.90 | -3.27 | 8.70 | 160.00 | 15.025 | .539 | 1.544 |
| 1645.12 | 1577.88 | -4.09 | 2.97 | 160.00 | 14.951 | .560 | 1.575 |
| 1674.66 | 1665.96 | -.52 | 34.08 | 180.00 | 14.912 | .542 | 1.443 |
| 1664.70 | 1652.11 | -.76 | 31.94 | 180.00 | 14.887 | .550 | 1.451 |
| 1651.34 | 1633.30 | -1.09 | 29.07 | 180.00 | 14.852 | .560 | 1.463 |
| 1638.39 | 1615.25 | -1.41 | 26.36 | 180.00 | 14.818 | .570 | 1.475 |
| 1623.96 | 1595.72 | -1.74 | 23.46 | 180.00 | 14.781 | .582 | 1.488 |
| 1608.47 | 1574.39 | -2.12 | 20.35 | 180.00 | 14.740 | .595 | 1.502 |
| 1593.23 | 1553.09 | -2.52 | 17.30 | 180.00 | 14.699 | .608 | 1.517 |
| 1579.41 | 1534.12 | -2.87 | 14.62 | 180.00 | 14.662 | .620 | 1.531 |
| 1562.04 | 1510.98 | -3.27 | 11.42 | 180.00 | 14.616 | .636 | 1.547 |
| 1546.24 | 1490.19 | -3.63 | 8.60 | 180.00 | 14.574 | .651 | 1.563 |
| 1531.56 | 1469.95 | -4.02 | 5.90 | 180.00 | 14.533 | .665 | 1.579 |
| 1514.50 | 1447.56 | -4.42 | 2.98 | 180.00 | 14.487 | .682 | 1.596 |
| 1568.77 | 1557.99 | -.69 | 34.67 | 200.00 | 14.520 | .635 | 1.446 |
| 1569.08 | 1556.74 | -.79 | 34.48 | 200.00 | 14.518 | .634 | 1.448 |
| 1554.50 | 1537.57 | -1.09 | 31.63 | 200.00 | 14.478 | .648 | 1.461 |
| 1542.61 | 1522.11 | -1.33 | 29.36 | 200.00 | 14.447 | .660 | 1.469 |
| 1524.37 | 1498.35 | -1.71 | 25.94 | 200.00 | 14.397 | .678 | 1.485 |
| 1513.91 | 1484.70 | -1.93 | 24.00 | 200.00 | 14.368 | .689 | 1.494 |
| 1493.44 | 1458.35 | -2.35 | 20.33 | 200.00 | 14.312 | .710 | 1.511 |
| 1475.66 | 1436.01 | -2.69 | 17.29 | 200.00 | 14.264 | .730 | 1.525 |
| 1458.18 | 1413.81 | -3.04 | 14.33 | 200.00 | 14.216 | .750 | 1.540 |
| 1440.66 | 1391.79 | -3.93 | 11.45 | 200.00 | 14.167 | .771 | 1.556 |
| 1420.44 | 1366.69 | -3.78 | 8.26 | 200.00 | 14.111 | .796 | 1.574 |
| 1400.22 | 1341.84 | -4.17 | 5.18 | 200.00 | 14.055 | .823 | 1.592 |
| 1380.82 | 1317.96 | -4.55 | 2.29 | 200.00 | 14.000 | .850 | 1.611 |
| 1468.01 | 1455.94 | -.82 | 35.01 | 220.00 | 14.126 | .745 | 1.445 |
| 1452.62 | 1437.01 | -1.07 | 32.30 | 220.00 | 14.084 | .763 | 1.455 |
| 1434.94 | 1415.24 | -1.37 | 29.24 | 220.00 | 14.035 | .785 | 1.467 |
| 1417.61 | 1394.05 | -1.66 | 26.33 | 220.00 | 13.986 | .807 | 1.480 |
| 1399.99 | 1372.70 | -1.95 | 23.45 | 220.00 | 13.937 | .830 | 1.492 |
| 1380.17 | 1348.72 | -2.28 | 20.29 | 220.00 | 13.880 | .858 | 1.508 |
| 1361.07 | 1325.71 | -2.60 | 17.34 | 220.00 | 13.826 | .885 | 1.522 |
| 1341.26 | 1302.34 | -2.90 | 14.42 | 220.00 | 13.769 | .916 | 1.537 |
| 1319.31 | 1276.56 | -3.24 | 11.28 | 220.00 | 13.706 | .951 | 1.554 |
| 1297.42 | 1251.03 | -3.58 | 8.26 | 220.00 | 13.643 | .987 | 1.572 |
| 1274.40 | 1224.42 | -3.92 | 5.22 | 220.00 | 13.576 | 1.029 | 1.591 |
| 1252.92 | 1199.96 | -4.23 | 2.50 | 220.00 | 13.514 | 1.069 | 1.608 |
| 1366.78 | 1356.03 | -.79 | 34.75 | 240.00 | 13.722 | .885 | 1.438 |
| 1354.79 | 1341.71 | -.97 | 32.79 | 240.00 | 13.687 | .903 | 1.445 |
| 1331.98 | 1314.77 | -1.29 | 29.19 | 240.00 | 13.621 | .938 | 1.460 |

TABLE II. *Experimental values of compressed liquid sound velocity, W_E , temperature T, and pressure, P. Sound velocity, W_c , and density, ρ , were computed from the PQT surface (ref. 7,8). Adiabatic compressibility, K_s , and specific heat ratio were computed from W_E and properties derived from the PQT surface.—Continued.*

| W_E m/s | W_c m/s | Δ % | P MPa | T K | ρ mol/L | K_s GPa ⁻¹ | γ |
|--------------|--------------|---------------|----------|--------|-----------------|----------------------------|----------|
| 1315.98 | 1296.06 | -1.51 | 26.74 | 240.00 | 13.574 | .965 | 1.470 |
| 1295.35 | 1272.20 | -1.79 | 23.70 | 240.00 | 13.513 | 1.000 | 1.484 |
| 1273.86 | 1247.34 | -2.08 | 20.62 | 240.00 | 13.449 | 1.039 | 1.499 |
| 1255.72 | 1226.66 | -2.31 | 18.13 | 240.00 | 13.395 | 1.074 | 1.511 |
| 1227.37 | 1194.90 | -2.65 | 14.42 | 240.00 | 13.311 | 1.131 | 1.530 |
| 1205.33 | 1169.98 | -2.93 | 11.61 | 240.00 | 13.244 | 1.179 | 1.546 |
| 1175.71 | 1137.32 | -3.27 | 8.06 | 240.00 | 13.155 | 1.247 | 1.567 |
| 1149.59 | 1108.82 | -3.55 | 5.10 | 240.00 | 13.075 | 1.312 | 1.587 |
| 1123.73 | 1081.19 | -3.79 | 2.35 | 240.00 | 12.997 | 1.382 | 1.606 |
| 1273.83 | 1265.36 | -.66 | 35.00 | 260.00 | 13.326 | 1.049 | 1.425 |
| 1254.47 | 1243.15 | -.90 | 32.12 | 260.00 | 13.267 | 1.086 | 1.436 |
| 1235.06 | 1221.13 | -1.13 | 29.34 | 260.00 | 13.207 | 1.126 | 1.448 |
| 1215.65 | 1199.46 | -1.33 | 26.68 | 260.00 | 13.148 | 1.167 | 1.459 |
| 1212.25 | 1195.70 | -1.37 | 26.22 | 260.00 | 13.137 | 1.175 | 1.462 |
| 1193.35 | 1174.68 | -1.56 | 23.71 | 260.00 | 13.079 | 1.218 | 1.472 |
| 1166.47 | 1145.01 | -1.84 | 20.29 | 260.00 | 12.995 | 1.283 | 1.489 |
| 1142.69 | 1118.92 | -2.08 | 17.38 | 260.00 | 12.920 | 1.344 | 1.505 |
| 1120.08 | 1094.75 | -2.26 | 14.79 | 260.00 | 12.850 | 1.407 | 1.518 |
| 1091.48 | 1063.69 | -2.55 | 11.58 | 260.00 | 12.758 | 1.492 | 1.538 |
| 1034.53 | 1004.14 | -2.94 | 5.84 | 260.00 | 12.576 | 1.685 | 1.576 |
| 1001.40 | 970.76 | -3.06 | 2.87 | 260.00 | 12.472 | 1.813 | 1.595 |
| 1181.52 | 1174.36 | -.61 | 34.56 | 280.00 | 12.911 | 1.258 | 1.416 |
| 1163.44 | 1154.56 | -.76 | 32.14 | 280.00 | 12.853 | 1.303 | 1.425 |
| 1142.60 | 1131.55 | -.97 | 29.40 | 280.00 | 12.786 | 1.359 | 1.436 |
| 1117.30 | 1104.02 | -1.19 | 26.23 | 280.00 | 12.703 | 1.430 | 1.451 |
| 1095.25 | 1080.16 | -1.38 | 23.57 | 280.00 | 12.631 | 1.497 | 1.463 |
| 1070.45 | 1053.86 | -1.55 | 20.75 | 280.00 | 12.550 | 1.577 | 1.476 |
| 1042.41 | 1024.19 | -1.75 | 17.70 | 280.00 | 12.456 | 1.675 | 1.493 |
| 1002.42 | 982.81 | -1.96 | 13.67 | 280.00 | 12.323 | 1.831 | 1.516 |
| 977.47 | 957.07 | -2.09 | 11.30 | 280.00 | 12.238 | 1.939 | 1.532 |
| 946.83 | 926.01 | -2.20 | 8.58 | 280.00 | 12.134 | 2.085 | 1.551 |
| 909.95 | 889.29 | -2.27 | 5.56 | 280.00 | 12.008 | 2.281 | 1.574 |
| 860.05 | 841.19 | -2.19 | 1.92 | 280.00 | 11.839 | 2.590 | 1.603 |
| 1098.21 | 1093.27 | -.45 | 34.75 | 300.00 | 12.506 | 1.503 | 1.401 |
| 1071.17 | 1063.71 | -.70 | 31.35 | 300.00 | 12.412 | 1.592 | 1.417 |
| 1055.73 | 1047.03 | -.82 | 29.49 | 300.00 | 12.358 | 1.646 | 1.425 |
| 1048.97 | 1040.11 | -.84 | 28.73 | 300.00 | 12.336 | 1.671 | 1.428 |
| 1017.21 | 1006.15 | -1.09 | 25.12 | 300.00 | 12.224 | 1.793 | 1.446 |
| 1010.40 | 999.13 | -1.12 | 24.40 | 300.00 | 12.201 | 1.821 | 1.449 |
| 989.11 | 976.70 | -1.25 | 22.14 | 300.00 | 12.125 | 1.912 | 1.461 |
| 976.05 | 963.07 | -1.33 | 20.80 | 300.00 | 12.079 | 1.971 | 1.468 |
| 965.74 | 952.41 | -1.38 | 19.78 | 300.00 | 12.042 | 2.019 | 1.474 |
| 944.24 | 930.41 | -1.46 | 17.73 | 300.00 | 11.966 | 2.126 | 1.485 |
| 942.26 | 928.64 | -1.45 | 17.57 | 300.00 | 11.959 | 2.136 | 1.487 |
| 908.52 | 894.37 | -1.56 | 14.54 | 300.00 | 11.838 | 2.321 | 1.505 |
| 904.05 | 889.83 | -1.57 | 14.15 | 300.00 | 11.821 | 2.347 | 1.509 |
| 876.16 | 861.82 | -1.64 | 11.83 | 300.00 | 11.720 | 2.521 | 1.525 |
| 868.38 | 853.89 | -1.67 | 11.20 | 300.00 | 11.690 | 2.572 | 1.531 |
| 847.35 | 833.36 | -1.65 | 9.61 | 300.00 | 11.614 | 2.719 | 1.543 |
| 827.58 | 813.96 | -1.65 | 8.17 | 300.00 | 11.541 | 2.869 | 1.555 |
| 792.52 | 780.58 | -1.51 | 5.83 | 300.00 | 11.413 | 3.164 | 1.575 |
| 787.49 | 775.71 | -1.50 | 5.50 | 300.00 | 11.394 | 3.209 | 1.579 |
| 748.57 | 739.26 | -1.24 | 3.19 | 300.00 | 11.250 | 3.597 | 1.603 |

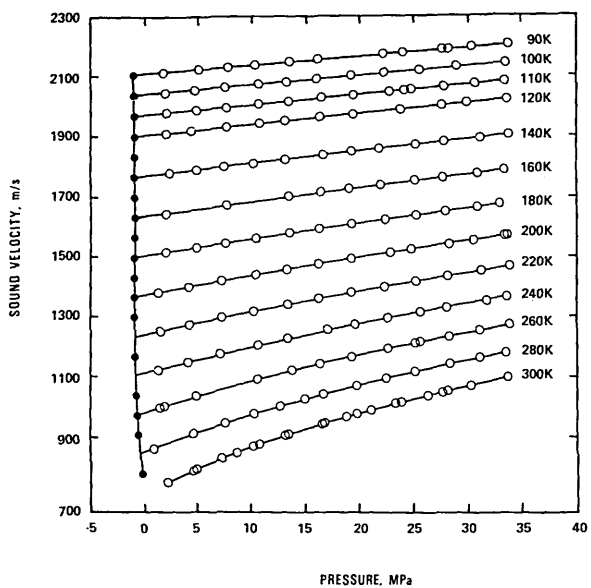


FIGURE 1. Sound velocity in compressed liquid propane as a function of pressure on isotherms. Closed circles are for saturated liquid.

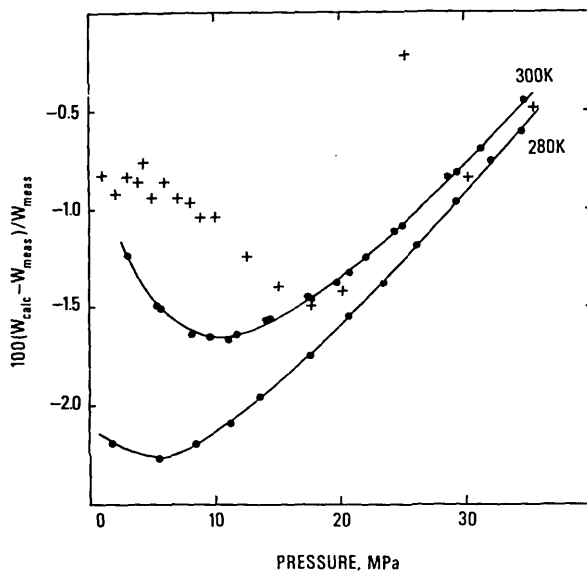


FIGURE 2. Deviation of Goodwin's calculated sound velocity relative to the data of Lacam for $T = 298.15$ K (+). For comparison, the deviation of Goodwin's calculated values relative to the measured values of this report are shown for $T = 280$ K and 300 K (•).

Models of Quasi-Steady and Unsteady Discharge from Plumbing Fixtures

Bal M. Mahajan,* Lawrence S. Galowin,* and Paul A. Kopetka*

National Bureau of Standards, Washington, DC 20234

August 20, 1980

Modeling methods are developed to predict the discharge characteristics of simulated simplified configurations for plumbing fixtures connected to horizontal drain branch piping. Computations are carried out to illustrate several methods of determining the effect of various loss coefficients of the drain connection, pipe length, pipe diameter, and friction factor. Solutions are obtained for the case of a fixture with a constant head (continuous refill) and a falling head (emptying of a sink). Numerical solution of the non-linear differential equation for the falling head case was obtained by the Runge-Kutta method. Discharge characteristics are presented for a range of flows and pipe diameter-to-length ratios representative of plumbing installations. The feasibility of developing predictive models for hydraulic characteristics of interconnected plumbing fixture and drainage piping systems is shown. The variations of efflux rate with the drain pipe diameter, length, and slope obtained from the assumed models are similar in trend to the available experimental data.

Key words: characteristics; discharge; drainage; flow; model; plumbing; quasi-steady; unsteady.

Nomenclature

A = cross-sectional area of the container
 a = cross-sectional area of the pipe
 d = pipe diameter
 f = pipe friction factor
 g = acceleration due to gravity
 h = instantaneous elevation of the free surface in the container above the center of the outlet of the drain
 h_0 = initial value of h
 h_e = initial elevation of the free surface in the container above the center of the outlet section of initial pipe or inlet section of drain pipe (see fig. 3)
 k_t = loss coefficient for the tank drain connection
 k_b = loss coefficient for the initial pipe bends and the initial pipe-exit pipe coupling
 R_c = loss coefficient for the sudden change in pipe diameter at the location where the initial pipe is coupled to the drain pipe
 $Q_i = a_i U_i$ = ideal efflux rate, i.e., the efflux rate when all head losses are neglected
 Q_e = efflux rate = $a_e U_e$
 u = instantaneous flow velocity
 U_e = mean velocity of flow in the exit pipe
 U_i = mean ideal velocity of flow in the exit pipe, that is the velocity when all head losses are neglected
 p = pressure

P_a = atmospheric pressure
 $s = \tan \alpha$ = slope or pitch of the drain pipe
 α = drain pipe slope angle
 $\beta = d_e/d_i$
 γ = specific weight of water
 $\phi = (1 + k_t + fL/d)$
 $\phi_1 = (k_t + K_b + f_1 L_1/d_i)$
 $\phi_2 = (f_e L_e/d_e + k_e)$

Subscript

1 refers to initial pipe
 e refers to drain pipe

Metric Conversion

feet \times 0.3048 = meters

1. Introduction

The mathematical modeling for determining the time dependent capacity characteristics of the drain-waste-vent plumbing system requires that the prescribed wastewater loads from a variety of fixtures and devices be determinable as the initial and boundary conditions. The development of models for calculation of time dependent discharge flows from plumbed fixtures as the forcing functions required to describe the loads on the drainage system is not well estab-

*Center for Building Technology, National Engineering Laboratory.

lished. The dynamics of the fixture discharge loading are mostly derived from experimental data sources that provide the combined loss effects as empirical factors. The theoretical developments are rendered difficult by the complex geometric configuration of the connecting elements of the fixture-drainage system (e.g. traps, elbows, tees, overflow drain, stopper flow area control, and branch drains) and by the turbulent flow conditions and secondary swirling. Further difficulties in a complete theoretical development are encountered due to the transition from full pipe flow to partially filled pipe flow downstream of the trap in the horizontal branch where changes in the size of elbow fittings, pipe diameter and slope often occur.

The dynamic transient characteristics of connected fixtures are generally assumed to be, a priori, independent of the downstream connections, drain or stopper geometry, elbow, fittings and the branch piping [1, 2].¹ Pressure variations within the drainage system (propagation of downstream conditions typical of incompressible low flow phenomena) are neglected in the usual methods for testing fixture performance in open air discharge tests at atmospheric pressure. The pressure variations, above and below atmospheric, occur in multi-story buildings as shown by Konen [3] and can influence fixture outflow.

Requirements for sizing the drain system as embodied in the plumbing codes in the U.S. are based upon the concepts of "fixture units." This traditional approach for water supply pipe sizing was extended to drainage systems, since the outflow very nearly equals inflow. This method, however, does not introduce the transient dynamics of the discharge flow phenomena and is applied as a "quasi-steady-state" loading for pipe sizing; it does, however, provide the significant input for peak water loads.

Test data comparing isolated open air fixture discharge characteristics with pipe connected fixtures show that the discharge curves are influenced by the connections to the drainage system; the predictive models should include the relevant constraints due to these connections. The model adopted in this study is for a horizontal drain carrying waste water from a fixture. The fixture discharge characteristics are found to be modified when losses due to piping and connections are introduced in the flow equations. The characteristics of interest are peak efflux rate, efflux rate-time history, maximum flow velocity in the horizontal drain, velocity-time history and the time required to empty the fixture. The parameters of interest for fixtures are the volume of water in the fixture, geometrical shape of the fixture, fixture to drain connections, drain exit conditions and physical characteristics of the drain pipe (i.e. diameter, length, slope, and friction factor).

This investigation is intended to be a parametric study only, varying each characteristic, one at a time; subsequent experiments are required to provide specific loss factors.

The plumbing fixtures are connected to the horizontal drains via connecting elements such as traps, downpipes, elbows, tees and other pipe fittings. The fixture discharge characteristics are influenced by the pressure losses and energy dissipation in these connecting elements, and by the physical characteristics of drain pipe. Predictive mathematical models and experimental validations are required to determine the effects of connecting elements and drain pipe characteristics on the fixture discharge parameters. The discharge characteristics of various plumbing fixtures with drain pipes of different physical characteristics (i.e. diameter, length and slope) was reported by Hanslin and Perrier [4] in an experimental investigation. Classical approaches based upon fundamentals and overly simplified models concerning the effects of the variables on the efflux rate from fixtures are available in basic hydraulic texts [5 and 6]. However, these studies for predicting the discharge characteristics of plumbing fixtures did not utilize representative models for effects of connector variables on the discharge characteristics.

This report illustrates the development of mathematical models for predicting the transient and quasi-steady state hydraulic discharge characteristics of a fixture coupled to the piping of a plumbing systems. This effort is the first step in developing the details of the dissipation effects from losses experienced in the flow within plumbing fixtures and connecting pipes. The next significant effort is required to develop a detailed analytical basis for the partially filled horizontal drain pipe. The effects of drain pipe parameters on the discharge characteristics of an open container, such as a lavatory or sink, under different flow conditions are presented. The number of variables for each model studied have been reduced in order to illustrate the most significant effects. For the steady state efflux rate from a constant head (continuous refill) container the effects of drain pipe parameters, taken one at a time, are shown. Also the solution for emptying a fixture based upon the instantaneous efflux rate from a falling head container (emptying fixture) is presented.

2. Unsteady flow drain—Falling head

Consider an open container with the uniform diameter drain pipe of length L fitted with a quick opening valve as shown in figure 1 to simulate a lavatory branch drainage pipe. Initially the container is full and the valve is closed. When the valve is rapidly opened, the available head will accelerate the fluid, the velocity of flow and rate of efflux will increase from zero to a maximum value. After attaining the maximum value, the flow velocity will decrease, because

¹ Figures in brackets indicate literature references at the end of this paper.

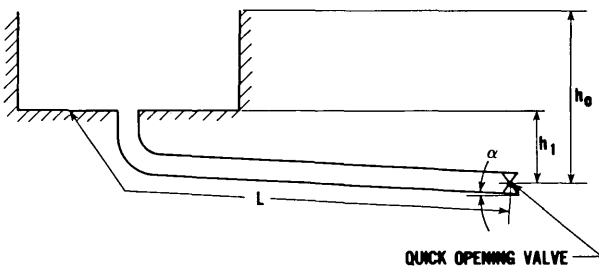


FIGURE 1. Lavatory-branch drain schematic.

the elevation of the water surface in the container will be decreasing as the water leaves the container. The final out-flow from the tank drain into the pipe would experience a discontinuity in the water surface area.

A one-dimensional unsteady flow analysis is adopted that leads to the non-linear equation of motion of the liquid discharged from a simulated lavatory-branch drainage pipe. The one-dimensional method assumes a uniform velocity across the flow area. Resistance and dissipation such as shear at the wall, turbulent mixing and drain vortex formation, and shedding losses are introduced through an empirical quasi-steady state set of constants. The losses are assumed to be proportional to the square of the velocity.

The equation of motion for the one-dimensional flow is:

$$\frac{L}{g} \frac{du}{dt} = h(t) - \phi u^2/2g \quad (1)$$

where: h = instantaneous elevation of the free surface above the center of the outlet section of the drain

u = instantaneous flow velocity in the drain pipe

ϕ = dissipation factor

The forcing term on the right hand side of eq (1) causing acceleration or deceleration of the fluid is dependent upon the decreasing head and the dissipation function. In this simplified model the losses accounted for are the friction in the pipe, and the loss coefficient for the tank to drain connection [5, 7]. The function is given by:

$$\phi = 1 + k_1 + fL/d \quad (2)$$

where: k_1 = loss coefficient for the tank drain connection

f = friction factor for the pipe taken as a constant factor for the range of Reynolds numbers

L/d = length to diameter ratio

The first term of eq (2) simply accounts for the decrease in total pressure head as a driving force due to the frictionless

conversion to the dynamic pressure. The ideal frictionless fluid case results from the assumption of $k_1=f=0$.

The relationship between the velocity u , at the drain of cross-sectional area, a , and the head, $h(t)$, in the tank of cross-sectional area, A , is obtained from the continuity equation,

$$\frac{dh}{dt} = -\frac{a}{A} u \quad (3)$$

The minus sign accounts for the falling head in the direction of the velocity.

The simultaneous eqs (1) and (3) are combined by assuming ϕ independent of time, differentiating (1), substituting (3) for dh/dt and rearranging the terms to yield

$$d^2u/dt^2 + \frac{\phi}{L} u \frac{du}{dt} + \frac{a}{A} \frac{g}{L} u = 0 \quad (4)$$

when

$$h < h_1, a/A = 1.$$

The initial conditions are:

$$t = 0, h = h_0, u = 0, \frac{du}{dt} = gh_0/L$$

with the last condition from eq (1). Equation (4) is recognized as a non-linear equation with constant coefficients when ϕ is assumed to take on quasi-steady values. The dissipation factors are functions of the local time dependent flow conditions; the terms of the function are taken as constant values over the flow regime, i.e. quasi-steady conditions, in this report. The solution by a numerical method based upon finite difference techniques is readily obtained.

The solution of eq (4) provides the flow velocity as a function of time. The numerical integration of the equation was obtained from a computer programmed Runge-Kutta method. A numerical integration method provides for adjustments in the value of a/A , k , and f at various points in the stepwise calculation, if it is desired to account for their variations. For a container with constant cross-sectional area, a/A changes only when the container empties and fluid is still present in the vertical section of the drain, i.e. when h is less than h_1 .

Example discharge velocity variations with time are shown in figure 2. In each of the three samples shown the acceleration from rest is very nearly constant over the initial time to attain the maximum flow. Since the velocity, u , is shown to be linear, it can be inferred from eq (3) that the height, h , varies with square of the time, t . The predicted discharge characteristics resemble the experimental discharge characteristics for various plumbing fixtures published in the literature [8 and 9]. To obtain quantitative

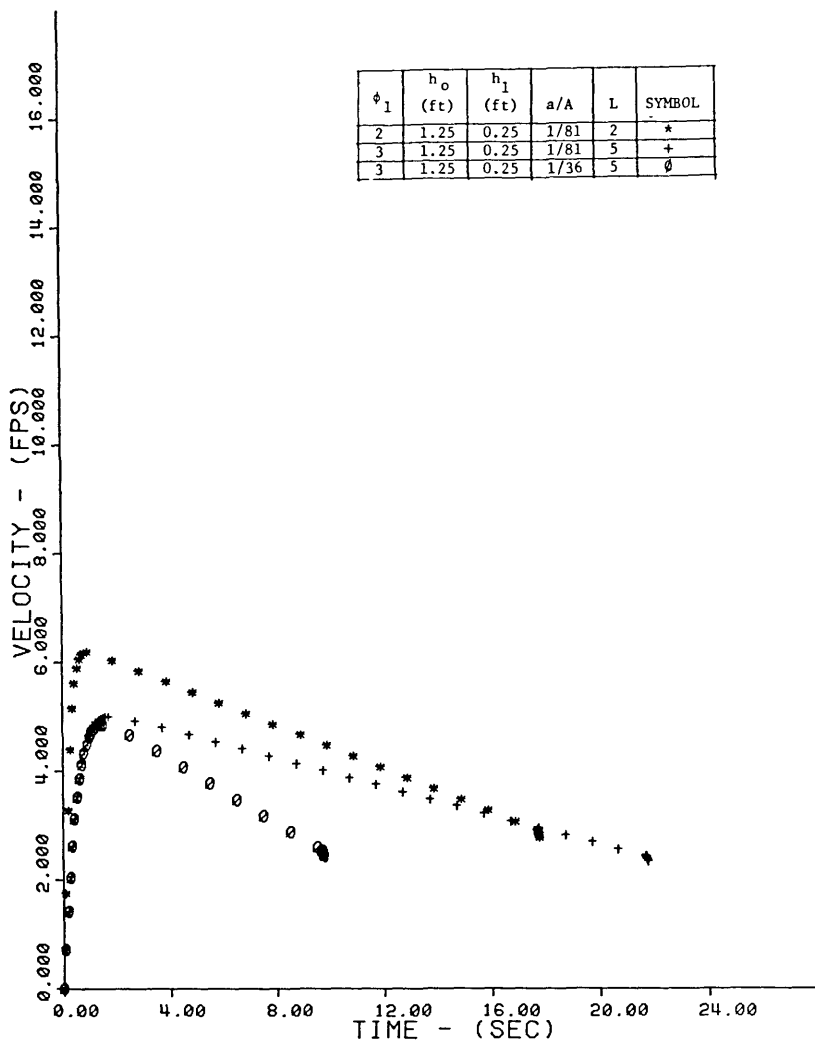


FIGURE 2. Discharge characteristics of a container-drainage system.

agreement between the predicted and experimental results it is necessary to determine the values of various loss coefficients from the experiments. As anticipated, the smallest time of discharge is obtained for the larger drain area ratio when holding the other terms constant; the maximum efflux velocity occurs with the lowest dissipation values.

3. Effects of drainage piping

The dependence of the discharge characteristics upon the interconnections of fixtures and devices with the piping system and the fittings at drain connections are investigated. The schematic for the steady state efflux from a con-

stant head (continuous refill) open container and drainage piping system is shown in figure 3. The assumption of constant head refill condition simplified the problem to a steady state analysis. The governing equations do not require the development of computer based numerical solutions of the differential equations. The effects of the variables of the piping system and drain connections can then be more readily evaluated in a parametric manner. The drainage system consists of an initial pipe of constant inside diameter d_i and length L_i , the initial pipe is coupled to a drain pipe of constant diameter d_e , length L_e and slope angle α . The mean velocity of the flow (U_e) in the drain pipe may be obtained by applying the modified Bernoulli equation between "O" and "e" as:

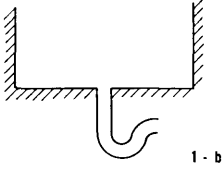
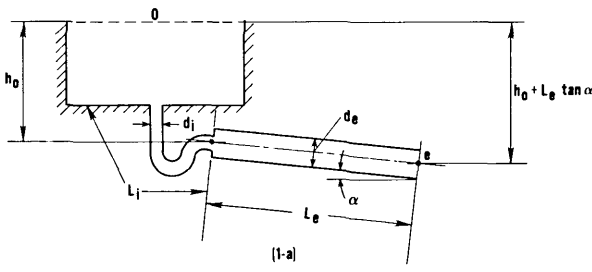


FIGURE 3. Constant head container drainage system.

$$P_o/\gamma + Z_o U_o^2/2g = \quad (5)$$

$$P_e/\gamma + Z_e + U_e^2/2g + \phi_1 U_1^2/2g + \phi_2 U_2^2/2g$$

with the conditions at inlet and outlet given by:

$$P_o = P_e = P_a; U_o = 0; Z_o - Z_e = h_e - L_e s$$

where $s = \sin \alpha$ and U_1 the velocity at the exit of the trap, i.e. the inlet of the drain pipe.

The dissipation functions are ϕ_1 and ϕ_2 where ϕ_1 is the function representing the losses at the tank to drain connection and in the initial pipe, and ϕ_2 is the function representing the losses at the step change in diameters and the horizontal drain. The equations are:

$$\phi_1 = (k_1 + k_b + f_1 L_1/d_1) \quad (6a)$$

$$\phi_2 = (f_e L_e/d_e + k_c) \quad (6b)$$

The continuity equation requires that for full bore pipe flow

$$U_1 = \beta^2 U_e, \quad \beta^2 = a_e/a_1 \quad (7a)$$

and the flow rate

$$Q_e = a_e U_e \quad (7b)$$

The condition of partially filled pipe flows is not considered here. A more extensive analysis is required to establish the transition condition for break away from full flow to partial filled flow.

The simplification of terms result in the velocity and flow rate equations

$$U_e = U_i [(1 + \frac{L_e s}{h_o}) / (1 + \beta^4 \phi_1 + \phi_2)]^{1/2} \quad (8a)$$

or

$$Q_e = Q_i \beta^2 [(1 + \frac{L_e s}{h_o}) / (1 + \beta^4 \phi_1 + \phi_2)]^{1/2} \quad (8b)$$

where the symbols are defined in the nomenclature.

Let U_r represent the mean velocity of flow and Q_r the efflux rate when the drainage system of the container of figure 3-a consists of just the initial pipe as shown in figure 3b. The expressions for U_r and Q_r , are obtained by letting L_e and ϕ_2 equal to zero and $\beta = 1$ as:

$$U_r = U_i / (1 + \phi_1)^{1/2} \quad (9a)$$

and

$$Q_r = U_r a_1 = Q_i / (1 + \phi_1)^{1/2} \quad (9b)$$

Equations (5) through (9) show the dependence of U_e and Q_e on the drain pipe variables (i.e., d_e , L_e , s , and f_e). For a falling head container where the conditions are slowly varying (i.e. area ratio of pipe to container less than 0.1), and may be considered as quasi-steady, these equations also give the instantaneous flow velocity and instantaneous efflux rate. The instantaneous flow velocity and efflux rate may be found by replacing h_o with the instantaneous value of the height, h , of the free surface in the container above the exit center of the cross-section of the initial pipe.

Using eqs (8a), (9a), (8b) and (9b), the quantities U_e and Q_e may be nondimensionalized as:

$$U_e/U_i = \{(1 + L_e s/h_o) / (1 + \beta^4 \phi_1 + \phi_2)\} \quad (10a)$$

$$U_e/U_r = \{(1 + L_e s/h_o) (1 + \phi_1) / (1 + \beta^4 \phi_1 + \phi_2)\} \quad (10b)$$

and

$$Q_e/Q_i = \beta^2 (U_e/U_i) = \beta^2 \{(1 + L_e s/h_o) / (1 + \beta^4 \phi_1 + \phi_2)\}^{1/2} \quad (11a)$$

$$Q_e/Q_r = \beta^2 (U_e/U_r) = \beta^2 \{(1 + L_e s/h_o) (1 + \phi_1) / (1 + \beta^4 \phi_1 + \phi_2)\}^{1/2} \quad (11b)$$

Equations (6) through (11) are applied to examine the effects of variations of any of the drain pipe variables on U_e and Q_e , as described in the following sections.

3.1 Effects of variations of the exit pipe diameter, d_e

For examining the effects of d_e on U_e and Q_e the following simplification can be made without loss of generality: (1) s is equal to zero; and (2) drain pipe is very smooth and has a short length so that the quantity $(f_e L_e / d_e)$ is negligible in comparison with the quantity k_c in dissipation function ϕ_2 that is $\phi_2 = k_c$.

The value of k_c is dependent upon the diameter ratio. For β less than 1 (i.e. $d_e < d_i$) the value of k_c has been experimentally determined by several researchers and may be found in the literature, typical values are shown in table 1. For $\beta > 1$ the relationship between k_c and β is given by the following expression:

$$K_c = (\beta^2 - 1)^2, \beta > 1 \quad (12)$$

Variations of the quantities U_e/U_i , U_e/U_r , Q_e/Q_i and Q_e/Q_r due to variations in d_e/d_i , for 3 different representative values of ϕ_1 , are presented in graphical form in figures 4 and 5.

TABLE 1

Values of loss coefficient, K_c , for sudden change in pipe diameter, taken from reference 7

| β^2 | 0.1 | 0.2 | 0.3 | 0.4 | 0.5 | 0.6 | 0.7 | 0.8 | 0.9 | 1.0 |
|-----------|------|------|------|------|------|------|------|------|------|------|
| K_c | 0.37 | 0.35 | 0.32 | 0.27 | 0.22 | 0.17 | 0.10 | 0.06 | 0.02 | 0.00 |

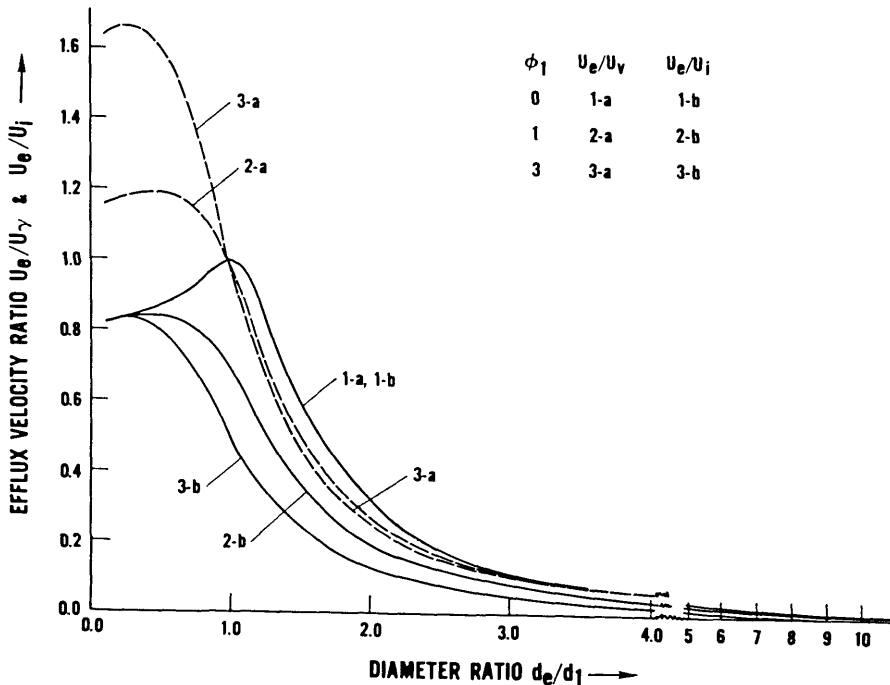


FIGURE 4. Water velocity ratio versus drain diameter ratio for efflux from a constant head container.

In the case of velocity ratios, in figure 4, it is seen that as the diameter ratio increases the velocity ratio decreases toward zero. As the drain pipe diameter increases for a fixed initial pipe diameter the velocity in the drain pipe will decrease or as the initial pipe diameter decreases for a fixed drain pipe diameter the velocity in the drain pipe will decrease. In figure 5 the efflux rate ratio Q_e/Q_r goes to unity after obtaining a local maximum. The ratio Q_e/Q_i reaches different asymptotic levels in the limit because the higher losses result in lower efflux rate as compared with the no loss condition required by Q_i . The critical value of diameter ratio β_c , at which Q_e/Q_r is maximum is determined by setting

$$\frac{d}{d\beta} (Q_e/Q_r) = 0 \quad (13a)$$

which yields

$$\beta_c = \sqrt{2} \quad (13b)$$

The value of Q_e/Q_i will also have the maximum value at β_c .

3.2 Effects of drain pipe length

To examine the effect of exit pipe length on the efflux the pipe slope, s , is assumed equal to zero and d_i equal to d_e .

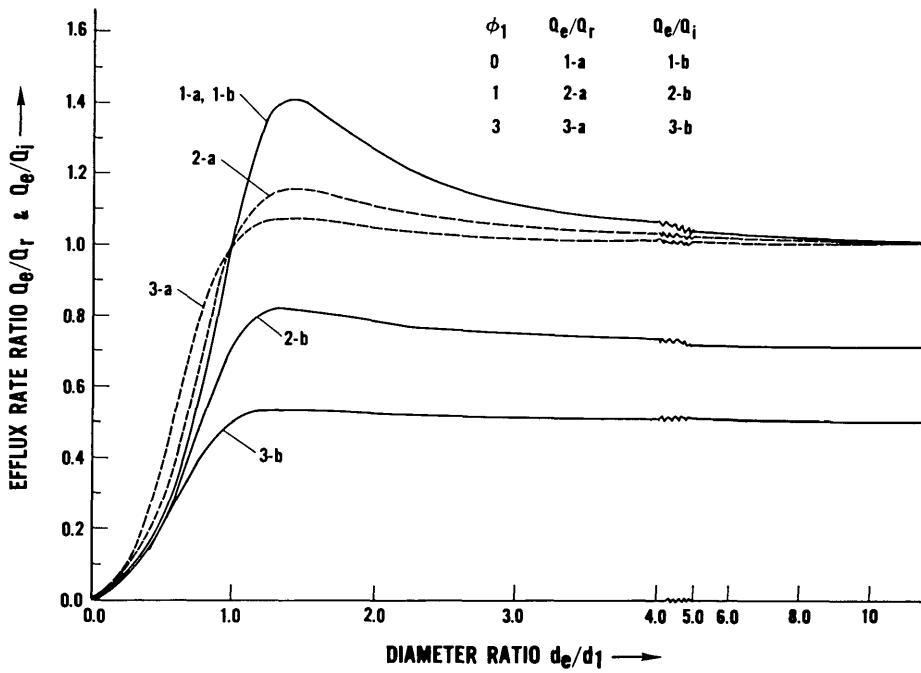


FIGURE 5. Efflux rate ratio versus drain diameter ratio for efflux from a constant head container.

By substitution and rearranging terms, the efflux rate equation becomes:

$$Q_e/Q_r = \{1/[1 + f_e L_e/d(1 + \phi_1)]\}^{1/2} \quad (14)$$

The variations of Q_e/Q_r due to variation in drain pipe length are presented in figure 6 for these representative values of ϕ_1 , and for one value of f_e (0.01).

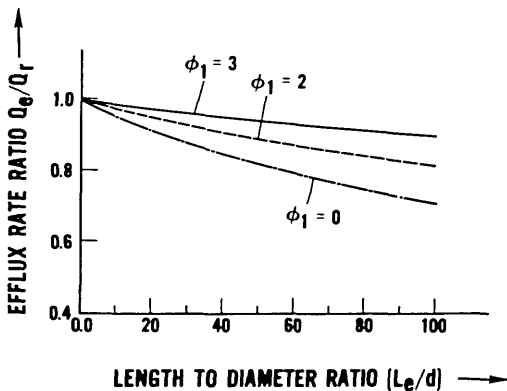


FIGURE 6. Efflux rate ratio versus drain length to diameter ratio for efflux from a constant head container.

3.3 Effects of drain pipe slope

For this case with diameters d_1 equal to d_e , the equations may be simplified to illustrate the effects of changes in pitch. If the drain pipe is short and very smooth, so that quantity $f_e L_e/d$ is negligibly small in comparison to the quantity $(1 + \phi_1)$, then the equations are further reduced:

$$Q_e/Q_r = U_e/U_r = [(1 + L_e s/h_o)/(1 + \phi_1)]^{1/2} \quad (15)$$

and

$$Q_e/Q_r = U_e/U_r = [1 + L_e s/h_o]^{1/2} \quad (16)$$

The variations of Q_e/Q_r due to variations in s , for three different values of L_e/h_o , are shown in figure 7. The increase in efflux with increasing pitch is consistent with the effect of the larger gravity force component that accelerates the flow. For the longer pipe a greater influence is obtained.

3.4 Effects of drain pipe friction factor

For examining only the effects of pipe friction on the flow it is assumed that s is equal to zero and d_1 is equal to d_e . The simplified equations become:

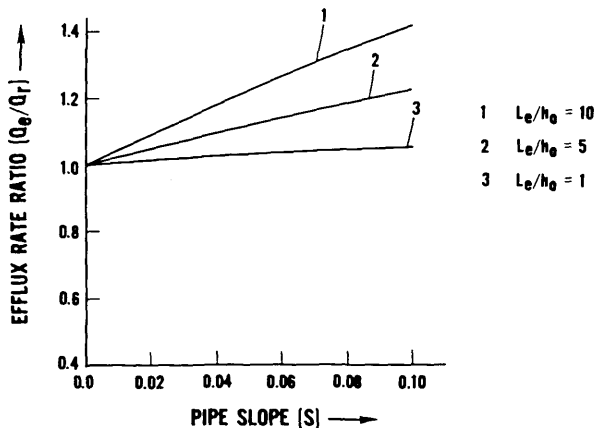


FIGURE 7. Efflux rate ratio versus pipe slope for efflux from a constant head container.

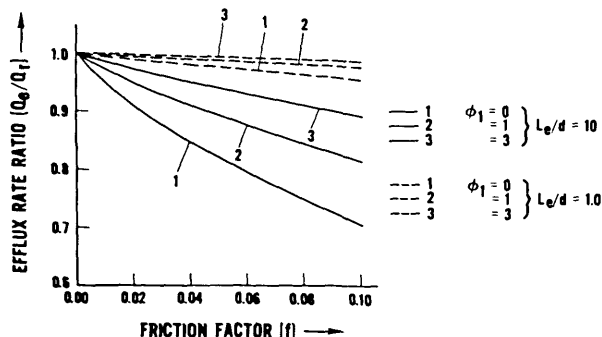


FIGURE 8. Efflux rate ratio versus pipe friction factor for efflux from a constant head container.

$$U_e/U_i = Q_e/Q_r = \{1 + L_e s/h_0\}^{1/2} \quad (17)$$

and

$$U_e/U_i = Q_e/Q_r = [(1 + \phi)/(1 + \phi + f_e L_e/d_e)]^{1/2} \quad (18)$$

The variations of Q_e/Q_r due to variation in f_e , for three different values of ϕ_1 and two values of L_e/d_e , are shown in figure 8.

It is noted that for a given value of the friction factor the ratio Q_e/Q_r increases with increasing ϕ_1 . The physical interpretation is that increased losses at the tank drain exit and the initial pipe section without the added length rapidly decrease Q_r . In terms of actual efflux rate, Q_e , the rate of flow is actually falling off with increased losses, but at a reduced rate as compared to Q_r .

4. Effects of drain variables on the fall of water level and time needed to empty a container

The depth of water and time required to empty the container of figure 3 is considered under quasi-steady flow conditions analogous to the region of slowly varying velocity shown in figure 2. When the free surface in the container is at height, h , above the center of the exit cross-section of the drain pipe, the instantaneous mean velocity, U_e , is given by the relationship:

$$U_e = [2gh / \{1 + \beta^4 \phi_1 + \phi_2\}]^{1/2} \quad (19)$$

The continuity eq (3) may be written as:

$$-dh = (a_e/A)U_e dt. \quad (20)$$

To determine the time required to empty the container, eq (20) should be solved rigorously by a succession of integrations, each over a small range of h and U_e , with approximate mean values for the time interval of the ϕ_1 and ϕ_2 values being used. This differs from the approach [6] where along a streamline of the flow the head varies with time and a solution is obtained based upon the exit pipe velocity. However, for examining the effects of the parameters on the time required to empty the container, the values of ϕ_1 and ϕ_2 are assumed constant and the equation is integrated in closed form following [6] with the initial condition $t=0, h=h_0$, which yields

$$t = 2(A/a_e) [(1 + \beta^4 \phi_1 + \phi_2)/2g]^{1/2} (\sqrt{h_0} - \sqrt{h}) \quad (21)$$

where t is the time required for the liquid level in the container to fall from h_0 to h . The time required to empty the container, t_e , is obtained by setting $h=h_1$ (see fig. 3).

The non-dimensionalized value with respect to t_e is given by:

$$t_e/t_r = (1/\beta^2) [(1 + \beta^4 \phi_1 + \phi_2)/(1 + \phi_1)]^{1/2}$$

where $t_r = (A/a_1)(2/g)^{1/2}(\sqrt{h_0} - \sqrt{h_1})(1 + \phi_1)^{1/2}$ is the time required to empty the container when the drainage system consists only of the initial pipe.

The equations indicate that the time required to empty the container will increase when ϕ_2 is increased and all of the other variables are kept constant. To examine the effect of the variation of d_e on the time required to empty the container, the quantity $f_e L_e/d_e$ may be assumed negligible in comparison with the quantity $(1 + \phi_e)$.

Another form of the equation is:

$$(h - h_1)/(h_0 - h_1) = 1 + \eta^2 t^2 / (h_0 - h_1) - 2\eta t \sqrt{h_0} (h_0 - h_1) \quad (23)$$

where

$$(\eta = (a_c/2A)[2g/(1 + \beta^4\phi_1 + \phi_2)]^{1/2}. \quad (24)$$

Equations (22) and (23) are presented graphically for different representative conditions, in figures 9 and 10, respectively. Higher efflux rates are anticipated (as has been shown) with lower dissipation values, and consequently the time for discharge is smaller. The maximum discharge value for $\beta = \sqrt{2}$ results in the minimum time value shown in figure 9.

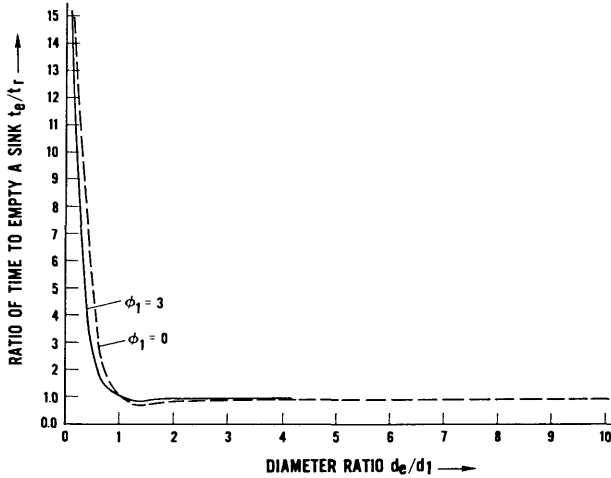


FIGURE 9. Time to empty sink versus drain diameter ratio.

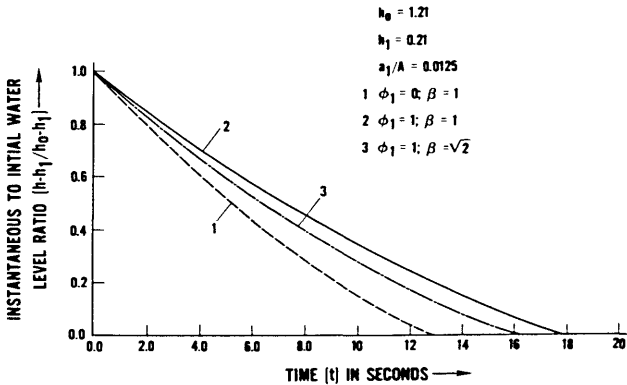


FIGURE 10. Water level ratio versus time for a falling head container.

5. Conclusions

Although the predictive models developed in this paper are for simple plumbing systems, the examples demonstrate the feasibility of developing mathematical models to predict the hydraulic characteristics and performance of complex plumbing systems. The theoretical discharge characteristics obtained by numerical methods of solution of the governing differential equation qualitatively resemble the experimental discharge characteristics for various fixtures reported by Wyly and Hintz [8] and Pink [9]. To obtain quantitative agreement between the predicted and experimental results it is necessary to determine the values of various loss coefficients from the experiments. The results presented showing the predicted variations of efflux rate with the diameter, length and slope of the drain pipe are similar to trends to the experimental results reported by Hanslin and Perrier [4].

6. References

- [1] Hunter, Roy B. Methods of estimating loads in plumbing systems. NBS Building Materials and Structures Report. BMS 65, 1940.
- [2] Eaton, H. N.; French, J. L. Fixture unit ratings as used in plumbing systems design. Housing and Home Finance Agency, Housing Reference Paper November 15, 1951.
- [3] Konen, T. P.; Jackson, T.; Fowell, A. J. The Evaluation of several plumbing drainage waste and vent systems. Davidson Laboratory, Stevens Institute of Technology, Report SIT-DL-74-1776 (December 1974).
- [4] Hanslin, R.; Perrier, F. The hydraulics of waste piping for sanitary appliances. Paper 12 presented at CIB W62 Seminar held in Stockholm, Sweden, 1974.
- [5] Rouse, H. *Elementary Mechanics of Fluids*, New York: John Wiley and Sons; Fifteenth edition; 1964.
- [6] Massey, B. S. *Mechanics of Fluids*, London: D. Van Nostrand; 1968.
- [7] John, J. E. A.; Haberman, W. *Introduction to Fluid Mechanics*, Englewood Cliffs, NJ: Prentice Hall, Inc.; 1971.
- [8] Wyly, R. S.; Hintz, D. Report on the discharge characteristics of household plumbing fixtures. NBS Report 1131, 1951.
- [9] Pink, B. J. Laboratory investigation of the discharge characteristics of sanitary appliances. Paper CP37/73 presented at the CIB W62 Symposium Research Seminar No. 2, held at the National Swedish Building Research Institute, Stockholm, 1973.

Transition Temperatures of the Hydrates of Na_2SO_4 , Na_2HPO_4 , and KF as Fixed Points in Biomedical Thermometry

R. L. Magin,^{*1} B. W. Mangum,² J. A. Statler,^{*3} and D. D. Thornton⁴

National Bureau of Standards, Washington, DC 20234

November 19, 1980

The hydrate transition temperatures of $\text{Na}_2\text{SO}_4 \cdot 10\text{H}_2\text{O}$ to Na_2SO_4 , $\text{KF} \cdot 2\text{H}_2\text{O}$ to KF, and $\text{Na}_2\text{HPO}_4 \cdot 7\text{H}_2\text{O}$ to $\text{Na}_2\text{HPO}_4 \cdot 2\text{H}_2\text{O}$ were established using ACS grade salts as 32.374 °C, 41.422 °C, and 48.222 °C, respectively. A simple and reliable procedure involving inexpensive materials was used to realize these transitions as temperature fixed points. Each transition temperature was attained within 30 minutes of hydrate initiation and remained constant to within ± 0.002 °C for more than 10 hours if the mixture was stirred. The established transition temperatures were sensitive at the 0.001 °C level to the amount of impurities, so the materials used should be of the highest quality available.

These systems fill a gap in the existing spectrum of temperature standards and should be useful in biomedical laboratories for calibrating thermometers.

Key words: biomedical thermometry; disodium hydrogen phosphate; fixed point; hydration temperature; potassium fluoride; salt hydrate; sodium sulfate; temperature calibration; temperature standard; thermistor; thermometer; transition temperature.

1. Introduction

Researchers in biomedical laboratories have become increasingly aware of the importance of temperature measurements as they strive to improve the overall quality of their tests and medical procedures. Currently, biochemists and physiologists are studying the temperature dependence of enzyme [1]⁵ and cellular [2] reactions, while in the clinic, hyperthermia is being examined as an adjuvant therapy in cancer treatment [3], hypothermia is being used to prolong cardiac surgery in infants [4], and cryogenic techniques are being studied for organ and tissue preservation [5].

At the same time, there have been dramatic developments in biomedical instrumentation that both require and provide greater accuracy in temperature measurement. For example, electronic digital thermometers equipped with a variety of specialized sensors [6] are now available which indicate temperature to a resolution of 0.01 °C. These new,

sophisticated instruments are being used to automate many test procedures. Valid measurements with these devices, however, require precise temperature control and accurate temperature measurement.

The only way to maintain thermometer accuracy, as with any other measurement, is through careful and well-documented calibrations at periodic intervals [7]. The purpose of this paper is to present a series of transition temperatures between the hydrates of inorganic salts as fixed points which can be used to calibrate thermometers quickly, easily, and with sufficient accuracy for most experimental purposes, *i.e.*, to about ± 0.01 °C [8]. These could be used in conjunction with existing temperature fixed points such as the ice point and the gallium melting point (National Bureau of Standards, SRM 1968) [9]. Many inorganic compounds form crystals in definite states of hydration. The phase transitions which occur when states of hydration change were suggested long ago as potential temperature fixed points [10]. Specifically, we report in this paper a detailed study of three hydrate transitions: (1) the anhydrous to decahydrate transition of sodium sulfate (Na_2SO_4), (2) the anhydrous to dihydrate transition of potassium fluoride (KF), and (3) the dihydrate to heptahydrate transition of disodium hydrogen phosphate (Na_2HPO_4). In addition, we present the results of a preliminary study which included three other salts (FeCl_3 , $\text{Zn}(\text{NO}_3)_2$, $\text{Na}_2\text{S}_2\text{O}_3$).

^{*}Guest Worker

¹ Present address: Department of Electrical Engineering, University of Illinois at Urbana-Champaign, Urbana, IL 61801

² Center for Absolute Physical Quantities, National Measurement Laboratory

³ Present address: Department of Chemistry, University of Southern California, Los Angeles, CA 90007.

⁴ Present address: Santa Barbara Research Center, Goleta, CA 93017.

⁵ Figures in brackets indicate literature references at the end of this paper.

1.1 History of the method

The idea of using the transition temperatures between hydrates of salts as fixed points for the calibration of thermometers was first suggested by M. Jeannel in 1866 [11], but received little attention until T. W. Richards rediscovered it in 1898 [12]. Richards and J. B. Churchill investigated several salt hydrate systems in considerable detail [13]. Their research demonstrated that such systems provide stable and reproducible temperature fixed points [14-19].

Although Jeannel had proposed using sodium acetate trihydrate, Richards began his research with sodium sulfate decahydrate, Glauber's salt. In 1898, he reported in a preliminary paper that Glauber's salt melts at 32.378 °C [12]. Then, in 1902, Richards and R. C. Wells carefully established the transition temperature for the complete dehydration of sodium sulfate decahydrate as 32.383 ± 0.001 °C [13]. H. C. Dickinson and E. F. Mueller, working at the National Bureau of Standards in 1907, confirmed these results when they obtained a value of 32.384 ± 0.003 °C on the International Hydrogen Temperature Scale [14] for the sodium sulfate transition temperature. As a result of these researches, the sodium sulfate decahydrate transition temperature and the freezing point of water [15] were the most accurately determined temperature fixed points of the time.

In 1899, Richards and Churchill outlined a research program to investigate the transition temperatures of nine salts which preliminary studies had shown were potentially useful as fixed points [16]. During the following twenty years, Richards and his coworkers established the transition temperatures between the hydrates of seven of those salts [17-21]. In addition to Richards, several other researchers have considered using salt hydrate transitions as fixed points in thermometry [22-24]. In 1930, H. O. Redlich and G. Loffler-Wein studied the transition temperatures of some ternary systems composed of two different salts and water using a platinum resistance thermometer [25]. In 1938, E. R. Washburn and W. J. Clem also used a platinum resistance thermometer to measure the metastable sodium sulfate heptahydrate to anhydrous salt transition temperature as 23.465 ± 0.004 °C [26]. These latter investigators all used the sodium sulfate decahydrate transition temperature to standardize their thermometers. Since 1938, a few papers have appeared concerning the use of salt hydrate transition temperatures as fixed points [27-30], but these are concerned only with attempts to use the sodium sulfate system and contribute little new information.

A list of the established salt hydrate transition systems with the reported transition temperatures is given in table 1. Although these systems cover the temperature range from 10 to 90 °C fairly well, there are some sizable gaps. Of particular significance to biomedical researchers is the gap from 35.36 to 50.664 °C. A literature search for salt hydrate

TABLE 1. Temperature fixed points established using transitions between different states of hydration of salts.

| Salt | Hydrate Transition States of Hydration | Transition Temperature (°C) | | |
|----------------------------------|---|-----------------------------|------------|----------|
| | | As Reported | On IPTS-68 | Ref. |
| Na ₂ CrO ₄ | 10H ₂ O-6H ₂ O | 19.529 | 19.522 | 19 |
| Na ₂ CrO ₄ | 10H ₂ O-4H ₂ O | 19.987 | 19.980 | 19 |
| Na ₂ SO ₄ | 7H ₂ O-0H ₂ O | 23.465 | 23.457 | 26 |
| Na ₂ CO ₃ | 10H ₂ O-7H ₂ O | 32.017 | 32.008 | 24 |
| Na ₂ SO ₄ | 10H ₂ O-0H ₂ O | 32.383 | 32.373 | 12,13,14 |
| Na ₂ CO ₃ | 10H ₂ O-1H ₂ O | 32.96 | 32.95 | 20 |
| Na ₂ CO ₃ | 7H ₂ O-1H ₂ O | 35.37 | 35.36 | 20 |
| NaBr | 2H ₂ O-0H ₂ O | 50.674 | 50.664 | 17 |
| MnCl ₂ | 4H ₂ O-2H ₂ O | 58.089 | 58.079 | 18 |
| SrCl ₂ | 6H ₂ O-2H ₂ O | 61.341 | 61.331 | 21 |
| SrBr ₂ | 6H ₂ O-2H ₂ O | 88.62 | 88.62 | 21 |

TABLE 2. Transitions potentially useful as fixed points.

| Salt | Hydrate Transition States of Hydration | Transition Temperature | |
|--|---|------------------------|-------|
| | | Reported (°C) | Ref. |
| Ba(C ₂ H ₃ O ₂) ₂ | 3H ₂ O-1H ₂ O | 24.7 | 31 |
| Na ₂ SeO ₄ | 10H ₂ O-0H ₂ O | 32 | 38 |
| Na ₂ HPO ₄ | 12H ₂ O-7H ₂ O | 35.0, 35.2 | 32,33 |
| Zn(NO ₃) ₂ | 6H ₂ O congruent | 36.1 | 34 |
| Ba(C ₂ H ₃ O ₂) ₂ | 1H ₂ O-0H ₂ O | 41 | 31 |
| KF | 2H ₂ O-0H ₂ O | 41 | 35 |
| Na ₂ S ₂ O ₃ | 5H ₂ O-2H ₂ O | 48.17 | 36,37 |
| Na ₂ HPO ₄ | 7H ₂ O-2H ₂ O | 40.0, 48.3 | 32,33 |
| Na ₃ PO ₄ | 12H ₂ O-unknown | 73.5 | 16 |
| Ba(OH) ₂ | 8H ₂ O-unknown | 78.0 | 16 |
| Na ₂ HPO ₄ | 2H ₂ O-0H ₂ O | 95.2, 95 | 32,33 |

transitions has produced the supplemental list shown in table 2 [31-38]. These systems were considered to have potential as temperature fixed points to fill the gaps in table 1.

2. Experimental method

2.1 Salt transitions

The hydrated crystal is a distinct phase of the water : salt binary system. The phase transition which occurs when a hydrated inorganic salt changes its state of hydration may be either congruent or incongruent depending on whether one or two solid phases are involved. In the former, the hydrated salt forms a saturated solution of the same composition. The liquid, solid and vapor phases ($P=3$) all have the same composition. Hence, the system may be considered to have but one component ($C=1$). In this instance, the Phase Rule [39], $F = C - P + 2$, predicts that the number of degrees of freedom (F) will vanish and a triple point will result. This is an unrealistic situation, of course, because it requires the salt to have the same vapor pressure as water at

the transition temperature in order for the vapor phase composition to be the same as that of the solid phase. Furthermore, if the starting material deviates from the crystal stoichiometry, the composition of the solution will change as the transition progresses, and with it, the temperature. This behavior can be understood by considering the phase diagram for the system $\text{Zn}(\text{NO}_3)_2 \cdot \text{H}_2\text{O}$ shown in figure 1 [34]. If a solution with composition 63.6 percent $\text{Zn}(\text{NO}_3)_2$ by weight is cooled from 40 °C, the hexahydrate will form, the composition of the solution will remain unchanged, and the temperature will remain at 36.1 °C during the entire hydration process. Thus, the phase transition is congruent and simulates the liquid-solid transition of a single pure material. If a solution of composition 60 percent $\text{Zn}(\text{NO}_3)_2$ by weight is cooled from 40 °C, however, it will not start forming the hexahydrate until the temperature is below 34 °C. Once crystallization starts, the solution becomes more dilute and the transition temperature decreases. Thus, a congruent transition is very sensitive to composition.

By contrast, a salt undergoing an incongruent transition exhibits four phases: liquid, vapor, and two solids in different states of hydration. In this case, the Phase Rule unequivocally predicts a quadruple point with zero degrees of freedom for the two component system. The presence of four phases lends a degree of compositional stability to the quadruple point as long as the system is sufficiently rich in salt to keep the solution saturated at the transition. This situation is illustrated by the phase diagram for $\text{Na}_2\text{SO}_4 \cdot \text{H}_2\text{O}$ shown in figure 2 [40]. In this case, any mixture of salt and solution with a total composition of 33.2 percent or more Na_2SO_4 cooled from 40 °C will start to form crystalline decahydrate at about 32.4 °C and will remain at that temperature until either the water (if the Na_2SO_4 composition is greater than 44.1 percent) or the anhydrous phase is exhausted.

As shown in figure 3, the system $\text{Na}_2\text{HPO}_4 \cdot \text{H}_2\text{O}$ exhibits two incongruent transitions [32,33,40]: one at about 48 °C from the heptahydrate to the dihydrate, and the other at about 35 °C from the dodecahydrate to the heptahydrate. At each of these transitions, the behavior of this system should be similar to that of sodium sulfate. It is possible for a single system to have both congruent and incongruent transitions, as illustrated by the phase diagram for $\text{KF} \cdot \text{H}_2\text{O}$ shown in figure 4 [35,40].

Two additional salt: water systems were surveyed: (1) the $\text{FeCl}_3 \cdot \text{H}_2\text{O}$ system, which has a phase diagram [40] qualitatively similar to that for $\text{Zn}(\text{NO}_3)_2 \cdot \text{H}_2\text{O}$, and (2) the sodium thiosulfate system, $\text{Na}_2\text{S}_2\text{O}_3 \cdot \text{H}_2\text{O}$, which has a very complex phase diagram [36,37,40] with several metastable phases in a small temperature range about 48 °C.

The six systems investigated are listed in table 3 along with the number of tests conducted on each salt and with the type of transition observed.

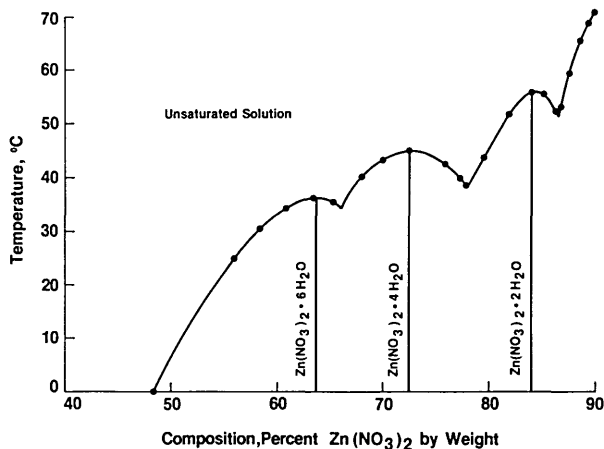


FIGURE 1. Phase diagram for the system $\text{Zn}(\text{NO}_3)_2 \cdot \text{H}_2\text{O}$. The melting points of the dihydrate, tetrahydrate, and hexahydrate are all congruent.

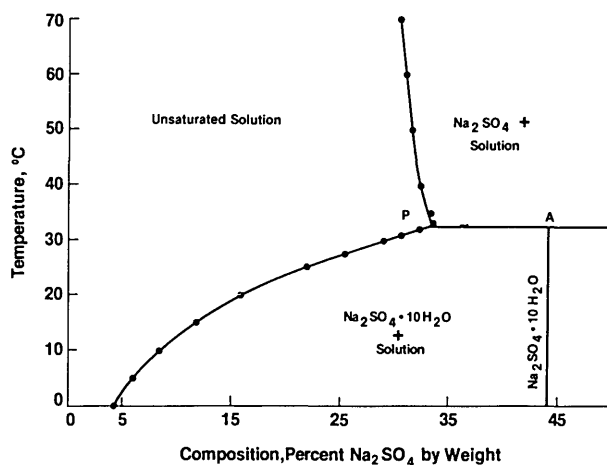


FIGURE 2. Phase diagram for the system $\text{Na}_2\text{SO}_4 \cdot \text{H}_2\text{O}$. The melting point of the decahydrate is incongruent.

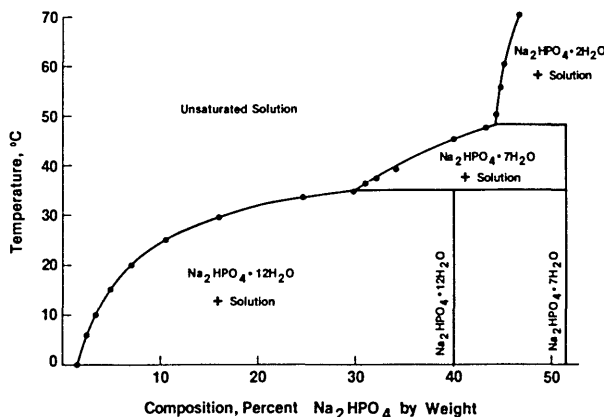


FIGURE 3. Phase diagram for the system $\text{Na}_2\text{HPO}_4 \cdot \text{H}_2\text{O}$.

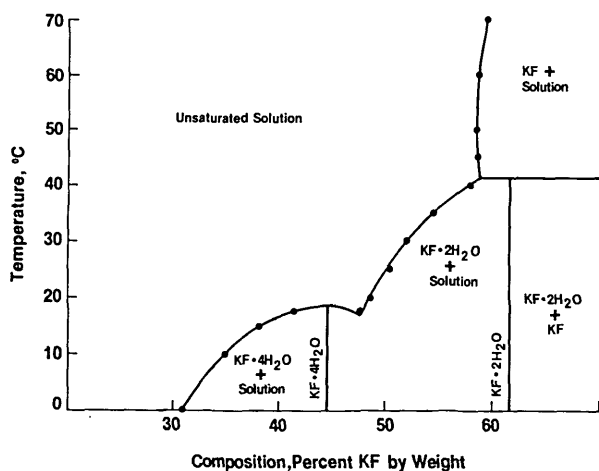


FIGURE 4. Phase diagram for the system KF:H₂O.

TABLE 3. Salt systems examined in this report.

| Salt Hydrate | Transition Temperature (°C) | Transition Type | Number of Tests |
|--|-----------------------------|-----------------|-----------------|
| Na ₂ SO ₄ ·10H ₂ O | 32.4 | incongruent | 19 |
| Zn(NO ₃) ₂ ·6H ₂ O | 36 | congruent | 5 |
| FeCl ₃ ·9H ₂ O | 37 | congruent | 3 |
| KF·2H ₂ O | 41.4 | incongruent | 20 |
| Na ₂ S ₂ O ₃ ·5H ₂ O | 48.2 | incongruent | 6 |
| Na ₂ HPO ₄ ·7H ₂ O | 48.2 | incongruent | 18 |

2.2 Salt samples

Analytical grade samples of each of the salts just discussed were obtained in 454 gram quantities from commercial (J. T. Baker, Fisher, Mallinckrodt) sources. In most cases, the samples came in glass bottles with lot number and lot analysis (or maximum impurity levels) on the bottle label. The KF·2H₂O samples were received in plastic bottles. Except for a few samples of sodium sulfate, all samples were obtained in crystalline form and were the highest purity grade available from each supplier. In table 4, the manufacturer's analysis of each lot studied is presented.

2.3 Thermometry

The temperature measuring apparatus used in this experiment employed six very stable and well-aged thermistors as sensing elements. The thermistors were connected in a series circuit with a constant current source and a thermostated, precision, ten kilohm resistor as shown schematically in figure 5. The resistance of each thermistor was determined in terms of the resistance of the precision "standard" resistor by measuring the potential differences

TABLE 4. Impurity analysis, supplied by manufacturer, of each lot used in the determination of the transition temperatures.

| Na ₂ SO ₄ ·10H ₂ O | Lot Number | | | |
|---|------------|------|------|------|
| | 092 | 558 | 026 | 824* |
| Contaminant (ppm) | | | | |
| Insoluble Matter | 20 | 20 | 50 | — |
| Chloride | 5 | 3 | 3 | — |
| Calcium, Magnesium | 20 | 30 | 40 | — |
| Phosphate | — | 5 | 4 | — |
| Free Acid (as H ₂ SO ₄) | — | 20 | 50 | — |
| Free Alkali | — | none | none | — |
| Nitrogen Compounds (as N) | 3 | 2 | 5 | — |
| Arsenic | 0.5 | 0.1 | 0.1 | — |
| Heavy Metals (as Pb) | 2 | 2 | 5 | — |
| Iron | <3 | 2 | 3 | — |

| KF·2H ₂ O | Lot Number | | | |
|---|------------|------|------|------|
| | 165 | 498 | 533 | 644 |
| Contaminant (ppm) | | | | |
| Iron | 10 | 2 | 10 | 10 |
| Chloride | 10 | 10 | 50 | 50 |
| Sulfate | 30 | 10 | 50 | 50 |
| Sulfite | 50 | 50 | — | — |
| Free Acid (as HF) | 1000 | 40 | 500 | 500 |
| Heavy Metals (as Pb) | 10 | 5 | 30 | 30 |
| Insoluble Matter | 20 | 50 | 200 | 200 |
| Free Alkali (as K ₂ CO ₃) | none | none | 1000 | 1000 |
| Silicofluoride (K ₂ SiF ₆) | 100 | 60 | 500 | 500 |
| Sodium | — | — | 200 | 200 |

| Na ₂ HPO ₄ ·7H ₂ O | Lot Number | | | |
|---|------------|-----|-----|-----|
| | 150 | 149 | 478 | 876 |
| Contaminant (ppm) | | | | |
| Insoluble Matter | 5 | 30 | 50 | 50 |
| Chloride | <5 | 10 | 10 | 10 |
| Sulfate | <20 | 20 | 50 | 50 |
| Heavy Metals (as Pb) | <5 | <5 | 10 | 10 |
| Iron | 5 | <5 | 10 | 10 |
| Nitrogen Compounds (as N) | 3 | 3 | 10 | 10 |
| Arsenic | 2 | 5 | 5 | 5 |

*Technical grade

across the thermistor (V_t) and the "standard" (V_s) in the sequence: $V_s, V_s, -V_s, -V_t$. The measuring current was 10 μ A in all measurements and calibrations. The potential differences were measured with a precision digital voltmeter (DVM) which had an input impedance in excess of $10^9 \Omega$ and a sensitivity of 10^{-7} V on the lowest scale. Five digits were displayed with a 160 percent overrange capability, so that the least-count resolution of the system in terms of temperature was about a quarter of a millidegree Celsius (m° C). The thermometer circuit was controlled by a mini-computer operating through an instrument bus so that the selection of sensors, thermistor current, and reading rates could be preprogrammed. The data were logged onto a magnetic disc at predetermined intervals during each experiment and later plotted as time-temperature profiles.

The thermistors were calibrated against a Standard Platinum Resistance Thermometer (SPRT) whose resistance was

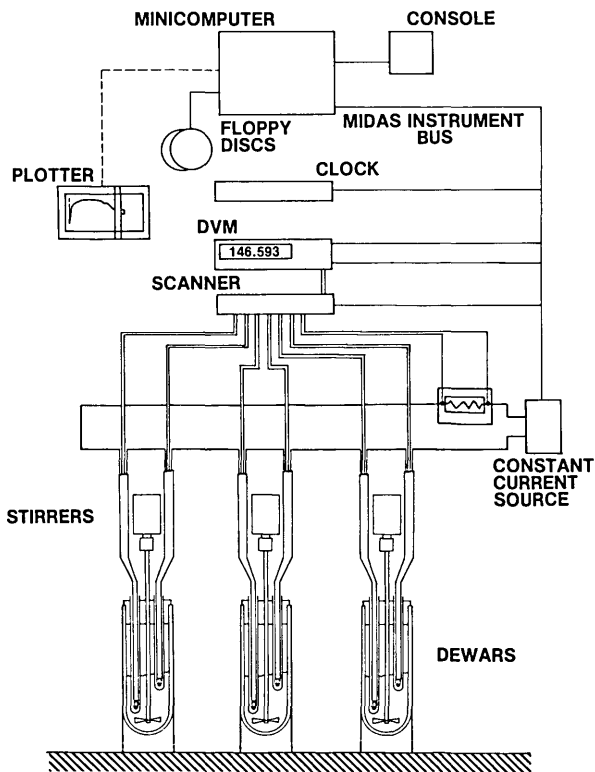


FIGURE 5. Temperature measurement system.

measured with a Cutkosky AC Resistance Bridge [41]. The calibration was done with thermistors and SPRT inserted into a copper block immersed in a well-stirred constant temperature bath. The temperature of the copper block was kept constant to within a few tenths of a millidegree Celsius. When the calibration data were fitted to a modified Steinhart equation [42], the largest deviation was one-half of a millidegree Celsius. The uncertainty in realizing IPTS-68 temperatures by the SPRT, in terms of the scale as maintained at NBS, was no more than ± 0.001 °C. The uncertainty in the thermistor measurements was about ± 0.001 °C as a result of (a) calibration, ± 0.0005 °C; (b) drift of thermistors between calibrations, ± 0.0002 °C; (c) limiting precision of the measurement, ± 0.0002 °C; and (d) possible variations in the self-heating of thermistors during measurement, ± 0.0001 °C. Thus, the overall uncertainty in the temperatures is ± 0.002 °C.

2.4 Apparatus

A diagram of the apparatus used for the transition temperature determinations is shown in figure 6. During the measurements, the salt hydrate mixture was contained in a 665 mL glass dewar covered by a styrofoam lid through

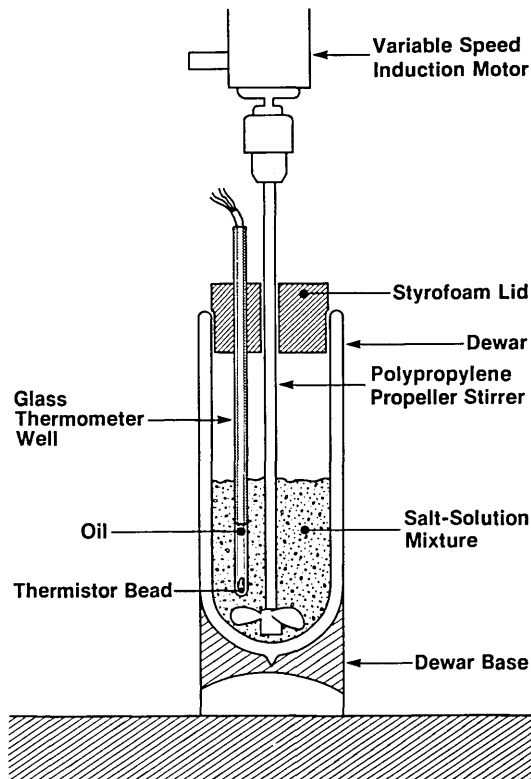


FIGURE 6. Schematic of experimental apparatus showing placement of thermistor temperature sensor and stirring propeller in 665 mL dewar.

which holes were drilled to accommodate a polypropylene propeller stirrer and glass thermometer wells. Normally, two thermistors in glass wells were used to measure the temperature of the mixture, one located 1 cm below the surface of the liquid and the other positioned 0.5 cm above the stirrer blades (3.5 cm below the surface of the liquid). The stirrer was driven at slow speed (200 rpm) by an induction motor with a variable speed drive attachment. Commutating motors could not be used as the electrical noise generated by the commutators affected the voltmeter readings.

A smaller, styrofoam-insulated beaker apparatus was used in a series of preliminary experiments. That apparatus consisted of a glass beaker (250 or 400 mL), plastic acrylic lid, and paired high density styrofoam sides (2 to 4 cm thick). The stirring method and the arrangement of glass thermistor wells were the same as that used in the dewar apparatus, except that commutating motors were used in these experiments.

2.5 Procedures

The transition temperature of each sample was determined in the following manner. The dewar, propeller stirrer, and glass wells were cleaned in tap water, rinsed with distilled

water, and soaked overnight in a dilute solution of HCl. Following the acid soak, the components were rinsed thoroughly with distilled water and allowed to drain. Bottles containing 454 g of a hydrated salt were partially immersed in a water bath whose temperature was approximately ten degrees Celsius above the transition temperature. Within one to two hours, the hydrated salt lost its waters of hydration, leaving a fine powder of the anhydrous salt (or lower hydrate) settled out of the solution. Occasionally, while the hydrated salt was being heated, the less hydrated form would crystallize in a hard mass on the bottom of the bottle, and it was necessary to break up this mass by very vigorous shaking. The water bath containing the bottle of the salt: Solution mixture was allowed to cool to a few degrees Celsius below the transition temperature. The hydration process was initiated when the bottle was removed from the bath and shaken. Normally this procedure would result in the onset of crystallization which could be detected by observing the sudden appearance of solid on the walls of the bottle. At this point, the bottle was opened and the contents poured into the dewar. The amount of residual salt remaining in the bottle was between five and ten grams.

On the few occasions when the transferred mixture had not begun to crystallize, the transition was initiated by adding a small quantity (1 to 5 g) of powdered hydrated crystals. When it was necessary to take this approach, we found that using finely powdered crystals generally resulted in a more rapid recalescence and a flatter plateau than did a few large crystals. As soon as the hydrating salt mixture was in the dewar, the thermometers and stirrer were inserted, the lid assembled and the stirrer started. The transition temperature was then monitored continuously for the next 15 to 30 hours.

An additional set of experiments investigated the characteristics of the sodium sulfate decahydrate transition under various conditions. In several of these experiments, the samples were prepared and solidified in 250 mL or 400 mL glass beakers, or in 265 mL dewars. Samples of 250 g or *ca.* 350–420 g were prepared by either driving off the waters of hydration, as described above, or by combining distilled water with anhydrous salt in the same proportion as that in the hydrated salt. In both cases, the mixture was brought to equilibrium several degrees Celsius above the transition temperature before cooling. After the mixture had supercooled about 0.3 °C below the transition temperature, the transition was initiated by adding 0.1 to 10 g of finely ground crystals of the appropriate hydrated salt.

3. Results

3.1 Preliminary survey

The six hydrated salts considered in the initial survey are listed in table 3. On the basis of the survey results, three of

the salt systems were not considered further in this study. The hydration transitions of the ferric chloride system, $\text{FeCl}_3 \cdot \text{H}_2\text{O}$, were difficult to initiate. Once the transition was started, the temperature did not maintain a plateau and displayed fluctuations of ± 0.03 °C. Although sodium thio-sulfate at first appeared stable, during subsequent trials the temperature displayed sharp, random changes of order 0.01 °C. Also, the measured values of the transition temperatures from different trials varied by as much as ± 0.1 °C. This behavior may reflect the presence of several metastable phases, as indicated by its phase diagram [36]. It was difficult to initiate the formation of zinc nitrate hexahydrate, although once started, the transition temperature appeared quite stable. Further difficulty in working with this system was encountered when lots labelled hexahydrate exhibited transitions at about 42 °C, indicating that the samples were of composition closer to that of the tetrahydrate (see fig. 1). Each of the three remaining salts appeared to exhibit sufficient stability and reproducibility to merit a more thorough examination.

During the preliminary experiments, a hydrated salt was sometimes reheated and the transition temperature measurements repeated. In these cases, the plateau temperatures determined were between 2 and 10 m°C less than the initial value. Because of this plateau temperature depression, probably due to contamination introduced during the first rehydration, only single runs on each hydrated salt were used for the principal temperature determinations.

3.2 Principal temperature determinations

In the principal set of experiments, time-temperature profiles were made of the hydration transitions of 57 samples of the three salts $\text{Na}_2\text{SO}_4 \cdot 10\text{H}_2\text{O}$, $\text{KF} \cdot 2\text{H}_2\text{O}$, and $\text{Na}_2\text{HPO}_4 \cdot 7\text{H}_2\text{O}$. The transitions were studied by monitoring the temperatures of the hydrating samples following the general procedure outlined above.

A typical time-temperature profile for each salt is shown in figure 7. The maximum temperature sustained during the "plateau period" was taken as the plateau temperature. The average plateau temperature, the number of samples, and the standard deviation of the temperatures for each lot are presented in table 5.

Both table 5 and figure 7 point out the substantial differences in behavior between the three salts. The sodium sulfate decahydrate was by far the most consistent. Nearly every profile was almost identical to that shown in figure 7. The recalescence period was so short that the sample temperature was within 0.002 °C of the plateau temperature in less than 15 minutes from the start of the transition. In the few instances in which the temperature of the mixture was not constant at the plateau temperature, it decreased by less than 0.002 °C in 20 hours.

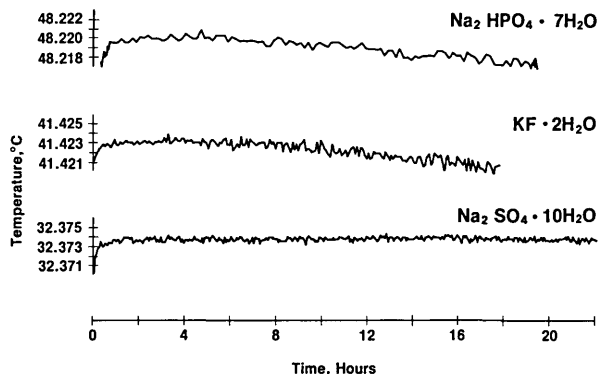


FIGURE 7. Typical temperature versus time profiles for the three reported salt transitions. Each transition was initiated at zero hours and the mixture stirred continuously.

TABLE 5. Results of principal temperature determinations, summarized by salt and lot.

| Salt Hydrate | Lot | Number of Samples | Average Plateau Temperature (°C) | Standard Deviation (°C) |
|---|-----|-------------------|----------------------------------|-------------------------|
| $\text{Na}_2\text{SO}_4 \cdot 10\text{H}_2\text{O}$ | 092 | 7 | 32.373 ₀ | 0.000 ₆ |
| | 558 | 3 | 32.373 ₂ | 0.000 ₈ |
| | 026 | 3 | 32.373 ₃ | 0.000 ₇ |
| | 824 | 6 | 32.373 ₈ | 0.001 ₁ |
| $\text{KF} \cdot 2\text{H}_2\text{O}$ | 165 | 5 | 41.393 ₈ | 0.001 ₄ |
| | 498 | 8 | 41.421 ₅ | 0.001 ₇ |
| | 533 | 6 | 41.383 ₅ | 0.001 ₀ |
| | 644 | 1 | 41.410 | — |
| $\text{Na}_2\text{HPO}_4 \cdot 7\text{H}_2\text{O}$ | 150 | 4 | 48.215 ₅ | 0.002 ₃ |
| | 149 | 8 | 48.216 ₅ | 0.004 ₂ |
| | 478 | 3 | 48.216 ₁ | 0.003 ₀ |
| | 876 | 3 | 48.221 ₇ | 0.005 ₁ |

The shape of the time-temperature profile for $\text{KF} \cdot 2\text{H}_2\text{O}$ was nearly as reproducible as that for sodium sulfate, i.e., it displayed a rapid recalcence followed by a gradual change in the temperature of less than 0.002°C over the next 20 hours. As can be seen from the data in table 5, however, the measured plateau temperatures varied considerably from lot to lot.

The most variable behavior within a lot was recorded for $\text{Na}_2\text{HPO}_4 \cdot 7\text{H}_2\text{O}$. The shapes of these profiles ranged from the eighteen hour plateau shown in figure 7 to those that remained constant for only a few hours before rapidly decreasing at up to $0.005^\circ\text{C}/\text{h}$. With the exception of one contaminated lot which has not been included, however, the temperature of hydration changed by less than 0.010°C over a period of at least 20 hours.

3.3 Immersion studies

In order to determine the best value for the hydration temperature of each salt, it was necessary to ascertain the effects of thermometer immersion into the stirred salt : solution mixture. Several experiments were conducted in which two or three thermometers were immersed to different depths in the mixtures. Figures 8, 9, and 10 show results for each salt which indicate an apparent top to bottom temperature gradient within the hydrating mixture of approximately 5°C . In addition, a single thermistor was used to probe vertically a $\text{Na}_2\text{HPO}_4 : \text{H}_2\text{O}$ mixture two hours after the transition had been initiated. The mixture was probed at three radial positions, 0.9 cm, 1.8 cm, and 2.7 cm, from

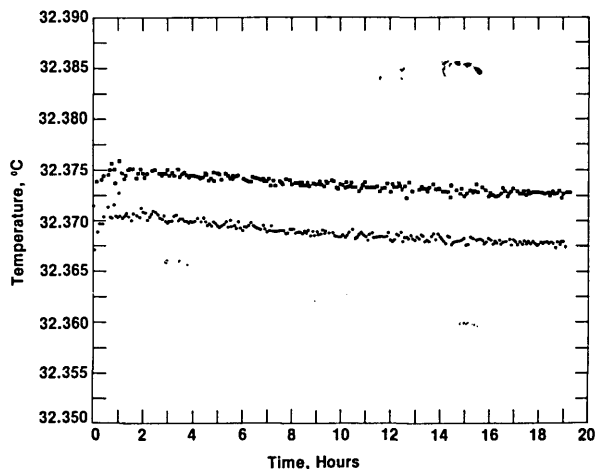


FIGURE 8. Temperature versus time profiles for the $\text{Na}_2\text{SO}_4 \cdot 10\text{H}_2\text{O}$ transition recorded at 3.5 cm (■) and 1.0 cm (●) below the surface of the mixture. The stirring propeller was located 4.0 cm below the surface.

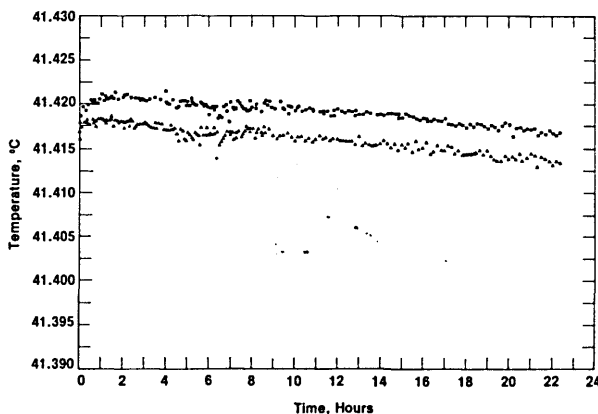


FIGURE 9. Temperature versus time profiles for the $\text{KF} \cdot 2\text{H}_2\text{O}$ transition recorded at 3.5 cm (■) and 2.5 cm (▲) below the surface of the mixture.

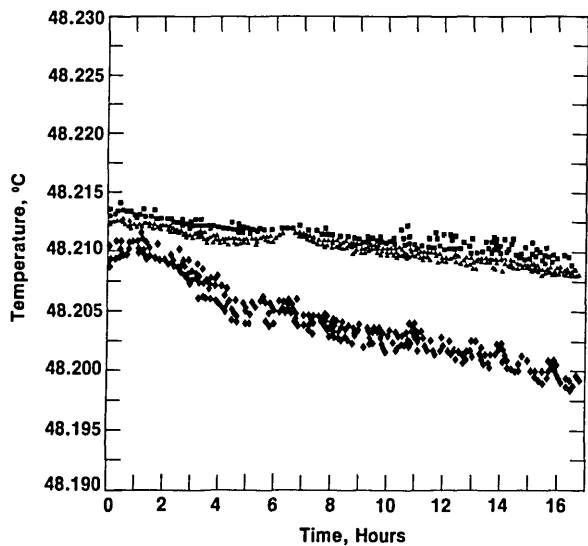


FIGURE 10. Temperature versus time profiles for the $\text{Na}_2\text{HPO}_4 \cdot 7\text{H}_2\text{O}$ transition recorded at 3.5 cm (■), 2.5 cm (▲), and 1.5 cm (◆) below the surface of the mixture.

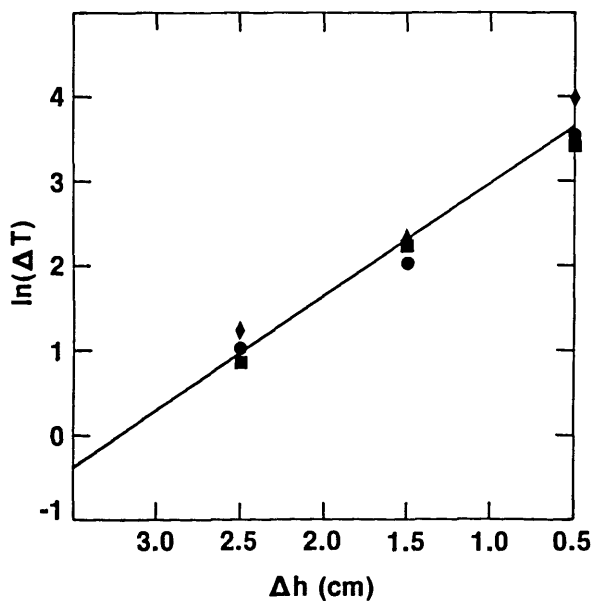


FIGURE 11. Temperature depression versus immersion depth at 0.9 cm (●), 1.8 cm (■), and 2.7 cm (◆) from the center of a 665 mL dewar containing a $\text{Na}_2\text{HPO}_4 \cdot 7\text{H}_2\text{O}$ transition.

the center of the 3.5 cm radius dewar. The results are shown in figure 11, where ΔT is the difference between the temperature of the thermistor at the indicated depth and that at a depth of 3.5 cm from the surface (0.5 cm above the stirrer). The roughly linear dependence of the data in figure 11

shows an exponential temperature change of the thermistor upon immersion in the thermistor well. These results indicate that the temperature at the depth at which the experimental measurements were made was depressed by heat loss to the surroundings by less than a millidegree Celsius.

3.4 Kinematic effects

The "true" transition temperature, whose stability is predicted by the Phase Rule, is maintained by the free energy available at the liquid-solid interface. Thus, in the non-equilibrium circumstance of constant heat loss from the vessel, there will be a temperature gradient from the interface through the liquid. Even if the mixture of solution and microcrystals is sufficiently well stirred to be homogeneous to a macroscopic thermometer, this average temperature is still somewhat lower than the interfacial temperature. The magnitude of the difference will depend upon the rate of heat loss, the thermal conductivity of the solution, the amount of surface available at the interface, as well as details in the mechanism of crystallization. Some of these effects were investigated in a series of experiments on the sodium sulfate : water system. This transition was studied at an ambient temperature of 24 °C in three vessels: a 665 mL dewar, a 265 mL dewar, and a 250 mL beaker insulated by styrofoam, as described previously. The data presented in figure 12 illustrate the results. The temperatures obtained in the large dewar, which should have the lowest heat loss, are the highest with the least fluctuations and longest period at maximum, while the converse is true for the temperatures measured in the relatively poorly insulated beaker.

To investigate the effect of interfacial area, we initiated sodium sulfate transitions with different quantities of decahydrate crystals of various sizes. It was difficult to control precisely the depth of supercooling for each of these experiments, so the results were not quantitative. Nevertheless, a few grams of granular decahydrate (crystals of 0.5 to 1 mm in diameter) resulted in a very extended recalescence and a rounded plateau, while a few grams of finely powdered material resulted in a rapid recalescence and a flat plateau.

An additional kinetic effect arises from the viscosity of the mixtures, due to heat generated as a result of mechanical stirring. The stirring is necessary to provide chemical and thermal homogeneity throughout the mixture. The plateau temperatures were not sensitive to stirring speeds between 200 and 600 rpm. At speeds less than 100 rpm, temperature gradients due to the settling of the more dense hydrate were observed and shorter plateau periods occurred, as shown in figure 13, whereas an increase in speed to greater than 600 rpm caused a step-like elevation in the measured temperature and a reversal in the direction of the transition.

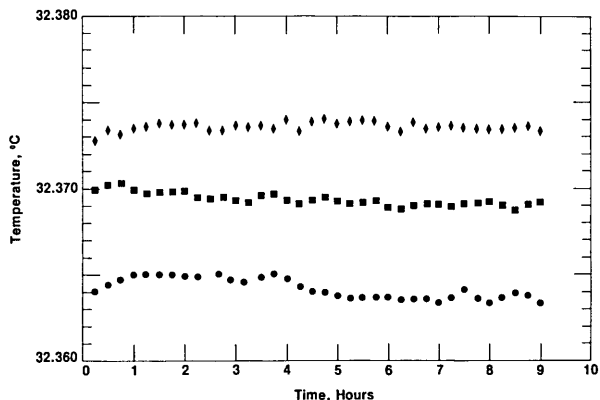


FIGURE 12. Temperature versus time profiles for the $\text{Na}_2\text{SO}_4 \cdot 10\text{H}_2\text{O}$ transition in a styrofoam insulated beaker (\bullet), a 265 mL dewar (\blacksquare) and a 665 mL dewar (\blacklozenge). Ambient temperature was 24 °C.

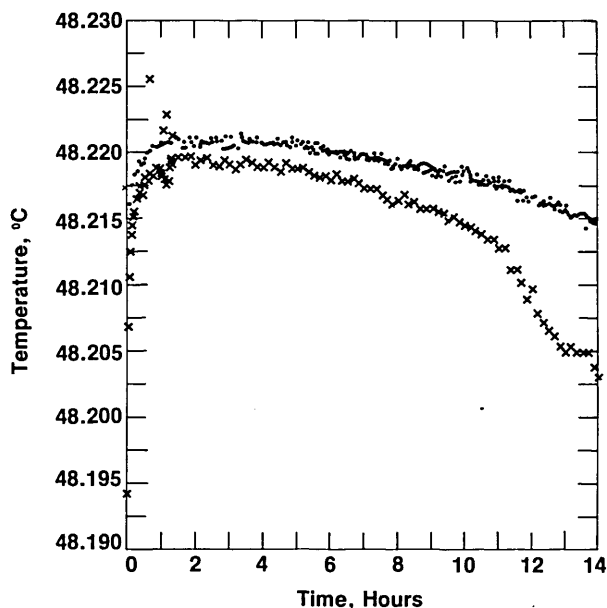


FIGURE 13. Temperature versus time profiles for the $\text{Na}_2\text{HPO}_4 \cdot 7\text{H}_2\text{O}$ transition at a slow, 100 rpm (\times), and fast, 300 rpm (\bullet), stirring speed.

4. Discussion of Results

4.1 Effects of atmospheric pressure

The experiments were conducted in air at atmospheric pressure, rather than at the quadruple point predicted by the Phase Rule. It is necessary, then, to assess the effects of pressure upon the transition temperature. This is given by

the Clapeyron equation for a first order phase transition [43]:

$$\frac{dP}{dT} = \frac{L}{T\Delta V} \quad (1)$$

where L is the latent heat of the transition, T is the transition temperature, and ΔV is the change in specific volume. We can apply this simple relation to each of the three salts with the following result:

| Salt | dT/dP , °C/Pa |
|---|--------------------|
| $\text{Na}_2\text{SO}_4 \cdot 10\text{H}_2\text{O}$ | $2 \cdot 10^{-8}$ |
| $\text{KF} \cdot 2\text{H}_2\text{O}$ | $23 \cdot 10^{-8}$ |
| $\text{Na}_2\text{HPO}_4 \cdot 7\text{H}_2\text{O}$ | $8 \cdot 10^{-8}$ |

As a check on these calculations, consider first a more sophisticated calculation which takes into account the fact that two components, and hence four phases, are involved in the first order transition. This generalized Clapeyron equation takes the form [44]

$$\frac{dP}{dT} = \frac{\Delta S_1 - A \Delta S_u}{\Delta V_1 - A \Delta V_u} \quad (2)$$

In this expression $\Delta S_{1,u} = S_{sol} - S_{1,u}$, where S_1 , S_u are the specific entropies of the lower and upper hydrates, S_{sol} is the specific entropy of the solution, and $\Delta V_{1,u} = V_{sol} - V_{1,u}$ where V_1 , V_u are the specific volumes of the lower and upper hydrates, and V_{sol} is the specific volume of the solution. The constant, A , is $A = (X_1 - X_{sol}) / (X_u - X_{sol})$, where X_u , X_1 , and X_{sol} are the weight fraction of upper hydrate, lower hydrate and the solution, respectively. These parameters are not available for all of the salts, but for sodium sulfate [45] the result is

$$\frac{dT}{dP} = 1.4 \cdot 10^{-8} \text{ °C/Pa} \quad (3)$$

Tammann [46] has measured this quantity experimentally for sodium sulfate and obtained

$$\frac{dT}{dP} = 0.5 \cdot 10^{-8} \text{ °C/Pa} \quad (4)$$

Note that the estimates formed using the Clapeyron equation, either eq (1) or its generalized version (2), are quite sensitive to the values of the specific volumes of the various phases.

Atmospheric pressure fluctuations over a period of 24 hours are typically less than ± 5 percent, so that differences in transition temperatures from sample to sample that might be attributable to such pressure changes are ± 0.10 m°C, ± 1.2 m°C, and ± 0.4 m°C for $\text{Na}_2\text{SO}_4 \cdot 10\text{H}_2\text{O}$, $\text{KF} \cdot 2\text{H}_2\text{O}$, and $\text{Na}_2\text{HPO}_4 \cdot 7\text{H}_2\text{O}$, respectively.

4.2 Effects of impurities

The effects of impurities can be estimated by assuming that they are present in sufficiently low concentrations that the laws for ideal dilute solutions apply. Then the depression in the transition temperature, ΔT , is given by [43]

$$\Delta T = \frac{RT^2}{L} (U_1 - U_s) \quad (5)$$

in terms of the gas constant, R , the heat of fusion, L , the transition temperature, T , and the impurity concentrations in the liquid, U_1 , and in the hydrated solid phase, U_s . The "cryoscopic constant," $k = RT^2/L$, can be evaluated [45] for each salt hydrate as 9.9 for $\text{Na}_2\text{SO}_4 \cdot 10\text{H}_2\text{O}$, 32.9 for $\text{KF} \cdot 2\text{H}_2\text{O}$, and 18.5 for $\text{Na}_2\text{HPO}_4 \cdot 7\text{H}_2\text{O}$. The value of this constant for $\text{Na}_2\text{SO}_4 \cdot 10\text{H}_2\text{O}$ has been calculated using a more precise expression [47] and it has also been measured experimentally [48]. Both values were found to be in very close agreement with the one given above.

Applying eq (5) to the specific samples used in this study would require determining the impurities and their concentration, as well as knowing the relative solubility of each impurity in both the solid and the liquid phases. Since there is no simple way to obtain this information, we have taken the approach that an upper limit can be estimated by using the manufacturer's lot analysis and by assuming that all impurities are only liquid soluble. On this basis we have obtained the following estimates, using eq (5), for the depression in the transition temperatures due to impurities.

| Salt Hydrate | Lot | Temperature Depression (m°C) |
|---|-----|------------------------------|
| $\text{Na}_2\text{SO}_4 \cdot 10\text{H}_2\text{O}$ | 092 | 1.5 |
| | 558 | 2.0 |
| | 026 | 2.5 |
| | 824 | >4.0 |
| $\text{KF} \cdot 2\text{H}_2\text{O}$ | 165 | 4.0 |
| | 498 | 1.0 |
| | 533 | 4.5 |
| | 444 | 4.5 |
| $\text{Na}_2\text{HPO}_4 \cdot 7\text{H}_2\text{O}$ | 150 | 2.1 |
| | 149 | 2.5 |
| | 478 | 3.4 |
| | 876 | 3.4 |

4.3 Stability and reproducibility of the transition temperature

From the results presented in table 5, it is apparent that the behavior of each system is quite distinctive, reflecting a different balance between heat generation by hydration and

heat loss to the surroundings. The transition temperature of disodium hydrogen phosphate is about 48.2 °C, or some 24 °C above ambient, while that of potassium fluoride is about 17 °C above ambient, and for sodium sulfate, it is only about 8 °C above ambient. In addition, the latent heat of hydration of $\text{Na}_2\text{HPO}_4 \cdot 7\text{H}_2\text{O}$ is only 172 J/g, while for $\text{KF} \cdot 2\text{H}_2\text{O}$ it is 262 J/g and for $\text{Na}_2\text{SO}_4 \cdot 10\text{H}_2\text{O}$ it is 245 J/g [45]. It is, therefore, no surprise that the Na_2HPO_4 exhibits a much longer recalcrescence, as well as a shorter plateau, than either of the other salts. This effect may also be important in determining the observed variation in transition temperature since the variation within lots shown in table 5 is of the same order of magnitude as the lot to lot variations. These results suggest that there is a correlation between impurities and observed transition temperature for Na_2HPO_4 , but the scatter of temperatures within a given lot is too great to establish this relationship precisely.

Potassium fluoride, on the other hand, shows much smaller variation of plateau temperature within a lot, though even this 0.002 °C variation could arise partly from variability in heat loss. Much more dramatic are the lot to lot variations, which in this case are as much as 0.04 °C. Although the listed impurities appear unable to account for these differences, it seems most likely that contamination is the cause. Potassium fluoride is a very reactive salt and it is difficult to control its level of purity.

Sodium sulfate is almost anomalously reproducible. On the basis of both pressure and impurity effects discussed above, variations of as much as 2 m°C appear possible. The variation actually observed was closer to 1 m°C.

5. Conclusions

The three salts studied exhibit transitions between different states of hydration for which the temperatures are stable to better than 2 m °C for several hours when the mixtures are well stirred in a dewar. The transition temperatures of all the salts are sufficiently reproducible for use as temperature fixed points, but since a few potassium fluoride temperatures were low by as much as 0.04 °C, the KF transition should not be used for high accuracy work. The disodium hydrogen phosphate transition temperatures, however, fell within a 0.007 °C range, while all the sodium sulfate transition temperatures were within a 0.002 °C range. The best values for the transition temperatures are: Na_2SO_4 to $\text{Na}_2\text{SO}_4 \cdot 10\text{H}_2\text{O}$ —32.374 °C, KF to $\text{KF} \cdot 2\text{H}_2\text{O}$ —41.422 °C, and $\text{Na}_2\text{HPO}_4 \cdot 2\text{H}_2\text{O}$ to $\text{Na}_2\text{HPO}_4 \cdot 7\text{H}_2\text{O}$ —48.222 °C.

We wish to thank H. S. Gutowsky and F. Dunn for suggesting improvements to the text.

6. References

- [1] Bowers, G. N. Jr.; Bergmeyer, H. U.; Moss, D. W. Provisional recommendations (1974) on IFCC methods for the measurement of catalytic concentration of enzymes. *Clin. Chem.* **22**: 384; (1976).
- [2] Bhuyen, B. K.; Day, K. J.; Edgerton, C. T.; Ogunbase, O. Sensitivity of different cell lines and different phases in the cell cycle to hyperthermia. *Cancer Res.* **37**: 3780; (1977).
- [3] *Cancer therapy by hyperthermia and radiation*, Proceedings of the 2nd International Symposium, Essen, Germany, June 2-4, 1977, ed. C. Streffer, Urban and Schwarzenberg, Baltimore 1978.
- [4] Moksi, H.; Dillard, D. H.; Crawford, E. W. Method of super-induced deep hypothermia for open-heart surgery in infants. *J. Thorac. Cardiovasc. Surg.* **58**: 262; (1969).
- [5] Popovic, V.; Popovic, P. *Hypothermia in biology and medicine*. New York: Grune and Stratton, Inc.; 1974.
- [6] Cromwell, L.; Weibell, F. J.; Pfeiffer, E. A. (eds). *Biomedical instrumentation and measurements, 2nd edition*. Englewood Cliffs, NJ: Prentice-Hall; 1980.
- [7] Mangum, B. W.; Thornton, D. D. The importance of temperature standardization in medicine. *Laboratory Management*. **1**: 32; (1978).
- [8] Magin, R. L.; Statler, J. A.; Thornton, D. D. The use of salt-hydrate transition temperatures as fixed points in biomedical thermometry, in 1979 *Advances in Bioengineering*, ASME, New York, 1979.
- [9] Thornton, D. D. The gallium melting-point standard: a determination of the liquid-solid equilibrium temperature of pure gallium on the International Practical Temperature Scale of 1968. *Clin. Chem.* **23**: 719; (1977).
- [10] Washburn, E. W., ed. *International critical tables of numerical data, physics, chemistry and technology*. Vol I. New York: McGraw-Hill Co., Inc; 1926. p. 66.
- [11] Jeannel, M. Note pour Servir a Phistoise de Pacetate le Soude. *Compt. Rend.* **62**: 834; (1866).
- [12] Richards, T. W. The transition temperature of sodic sulphate, a new fixed point in thermometry. *Am. J. Sci. Ser. 4* **6**: 201; (1898).
- [13] Richards, T. W.; Wells, R. C. The transition temperature of sodic sulphate referred anew to the international standard. *Proc. Am. Acad. Arts. Sci.* **38**: 431; (1902).
- [14] Dickinson, H. C.; Mueller, E. F. The transition temperature of sodium sulphate. *J. Am. Chem., Soc.* **29**: 1381; (1907).
- [15] Burgess, G. K. The present status of the temperature scale. *Orig. Comm. 8th Intern. Congr. Appl. Chem.* **22**: 53; (1911)
- [16] Richards, T. W.; Churchill, J. B. The use of the transition temperature of complex systems as fixed points in thermometry. *Proc. Am. Acad. Arts Sci.* **34**: 277; (1899).
- [17] Richards, T. W.; Wells, R. C. The transition temperature of sodic bromide: a new fixed point in thermometry. *Proc. Am. Acad. Arts Sci.* **41**: 455; (1906).
- [18] Richards, T. W.; Wrede, F. The transition temperature of manganous chloride: a new fixed point in thermometry. *Proc. Am. Acad. Arts Sci.* **43**: 343; (1907).
- [19] Richards, T. W.; Kelley, G. L. The transition temperatures of sodium chromate as convenient fixed points in thermometry. *Proc. Am. Acad. Arts Sci.*, **47**: 171; (1911).
- [20] Richards, T. W.; Fiske, A. H. On the transition temperatures of the hydrates of sodium carbonate as fixed points in thermometry. *J. Am. Chem. Soc.* **36**: 485; (1914).
- [21] Richards, T. W.; Yngre, V. The transition temperatures of strontium chloride and strontium bromide as fixed points in thermometry. *J. Am. Chem. Soc.* **40**: 89; (1918).
- [22] Meyerhoffer W.; Saunders, A. P. Ein Neuer Fixpunkt für Thermometer Vorshlag für Eine Normalzimmertemperatur. *Zeit. Phys. Chem.* **27**: 367; (1898).
- [23] Geer, W. C. Thermostats and thermoregulators. *J. Phys. Chem.* **6**: 85; (1902).
- [24] Wells, R. C.; McAdam, D. J. Phase relations of the system sodium carbonate and water. *J. Am. Chem. Soc.* **29**: 721; (1907).
- [25] Redlich, O.; Löffler-Wien, G. Neue Temperaturfixpunkte. *Zeit. Electrochem.* **36**: 716; (1930).
- [26] Washburn, E. R.; Clem, W. J. The transition temperature of sodium sulfate heptahydrate. *J. Am. Chem. Soc.* **60**: 754; (1938).
- [27] Hole, J. Thermometer standardizing with sodium sulphate. *Chem. and Met. Eng.* **52**(6): 115; (1945).
- [28] Constable, F. H.; Cansever, W. Variations in apparent transition point of sodium sulphate. *Rev. Faculte Sci. Univ. Istanbul*, **15**: 47; (1950).
- [29] Masuda, S. Transition temperature of $\text{Na}_2\text{SO}_4 \cdot 10\text{H}_2\text{O}$ as a temperature scale calibration point. *Kanto Gakuin Daigaku Kogakubu Kenkyu Hokoku*, **11**(1): 7; (1966).
- [30] Masuda, S.; Mieko, O. Transition temperature of $\text{Na}_2\text{SO}_4 \cdot 10\text{H}_2\text{O}$ as a standard temperature point II. *Kanto Gakuin Daigaku Kogakubu Kenkyu Hokoku*, **13**(1): 29; (1968).
- [31] Walker, J.; Fyffe, W. A. The hydrates and the solubility of barium acetate. *J. Chem. Soc.* **83**: 173; (1903).
- [32] Menzies, A. W. C.; Humphrey, E. C. Disodium monohydrogen phosphate and its hydrates: their solubilities and transition temperatures. *Orig. Com. 8th Intern. Congr. Appl. Chem.* **2**: 175; (1912).
- [33] Hammick, D. L.; Goadby, H. K.; Booth, H. Disodium hydrogen phosphate dodecahydrate. *J. Chem. Soc.* **117**: 1589; (1920).
- [34] Ewing, W. W.; McGovern, J. J.; Mathews, G. E. The temperature composition relations of the binary system zinc nitrate—water. *J. Am. Chem. Soc.* **55**: 4827; (1933).
- [35] Jatlov, V. S.; Poljakova, E. M. Equilibrium in the systems $\text{KF} \cdot \text{H}_2\text{O}$ and $\text{KHF}_2 \cdot \text{H}_2\text{O}$. *Zhur. Obs. Khimi.* **8**: 774; (1938).
- [36] Young, S. W.; Burke, W. E. Further studies on the hydrates of sodium thiosulfate. *J. Am. Chem. Soc.* **28**: 315; (1906).
- [37] Cramer, J.S.N. Sodium thiosulfate for standardization in thermometry. *Chem. Weekblad.* **28**: 316; (1931).
- [38] Funk, R. Über die Natriumsalze einiger, der Schwefelsäure analoger zweibasischer Säuren. Studien über die Löslichkeit der Salze VI. *Ber. Dtsch. Chem. Ges.* **33**: 3696; (1900).
- [39] Ricci, J. E. *The phase rule and heterogeneous equilibrium*. New York: D. Van Nostrand; 1951.
- [40] Seidell, A. (ed) *Solubilities of inorganic and metal organic compounds*. Vol. 1, 3rd edition. New York: D. Van Nostrand; 1940.
- [41] Cutkosky, R. D. An A-C Resistance-Thermometer Bridge. *J. Res. Nat. Bur. Std. (U.S.) Eng. and Instr.* **74C**(1 & 2): 15-18; 1970 January-June.
- [42] Steinhart, J. S.; Hart, S. R. Calibration curves for thermistors. *Deep-Sea Research.* **15**: 497; (1968).
- [43] Maron, S. H. and Prutton, C. F. *Principles of physical chemistry* New York: Macmillan; 1959.
- [44] Donnan, F. G.; Haas, A. (eds). *A commentary on the scientific writings of J. Willard Gibbs. Vol. I Thermodynamics*. Chapter 6, The phase rule and heterogeneous equilibrium. G. W. Morse. New Haven: Yale University Press; 1936.
- [45] Weast, R. C. (ed) *Handbook of chemistry and physics, 55th edition*. Cleveland: CRC Press; 1975.
- [46] Tammann, G. *the states of aggregation, The changes in the state of matter and their dependence upon pressure and temperature*. New York: D. Van Nostrand; 1925.
- [47] Fernandez-Prini, R.; Prue, J. E. Salt cryoscopy: the depression of the sodium sulphate decahydrate transition temperature by dissolved solutes. *J. Chem. Soc. (A)*: 1974; (1967).

[48] Briggs, C. C.; Freemont, P. S.; Lilly, T. H. Effect of solids on the sodium sulphate decahydrate transition temperatures. *J. Chem. Soc. (A)*: 2603; (1971).

A Game-Theoretic Model of Inspection-Resource Allocation*

Martin H. Pearl[†] and Alan J. Goldman[†]

National Bureau of Standards, Washington, D.C. 20234

July 2, 1980

This paper presents a generalization of a game-theoretic model, first described in an earlier paper, of the relationship between an inspectee who may decide to "cheat" or not, and an inspector whose task it is to minimize the expected gain that the inspectee achieves by cheating. When cheating is detected by the inspector, a penalty is assessed against the inspectee. The generalized model permits imposing a relationship between the level of the penalty to the inspectee when he/she is caught and the value to the inspectee of not being caught when he/she is cheating. The solution of the game takes on different forms depending on whether or not the inspector's resources are sufficient to make the detection of cheating likely.

Key words: Inspection; mathematical model; regulation; theory of games.

1. Introduction

In an earlier paper [2],¹ the authors presented three simple mathematical models of game-theoretic type, with the aim of exploring "strategic" aspects of the inspector-inspectee relationship. These models arose in the context of a study performed for the NBS Office of Weights and Measures, and were tailored to fit the specific situation encountered there. We also discussed a number of possible directions for generalizing the models in order to make them relevant to other situations involving an inspector-inspectee relationship.

Shortly thereafter, the opportunity arose to investigate the inspector-inspectee relationship inherent between the Internal Revenue Service and taxpayers. Indeed, the direct impetus for the current study was an attempt to apply the models of [2] to the problems faced by the Audit Division of IRS when trying to promote compliance by taxpayers to the Income Tax Regulations [1]. In each of the models of [2], the penalty imposed on the inspectee when cheating is detected by the inspector was assumed to be the same in all cases (P). For the purposes of [1], we were obliged to investigate the consequences of dropping that assumption: in particular, of relating the level of the penalty to the magnitude of the gain from cheating (if undetected). The present paper's model is sufficiently general to permit introducing such a relationship.

The definitions, notation, terminology, etc. used in [2] are retained here. Although it has been necessary to repeat parts of the earlier paper in order to make this one self-contained, this has been kept to a minimum. For this reason we recommend that the reader become familiar with the earlier paper, whose sections 1 and 2 describe the general aim of this line of research as well as (on p. 192) the motivation for the extension treated here.

2. Formulation of the Model

This mathematical model takes the form of a 2-player zero-sum game. The "players" are the *inspector* (an aggregate representing the inspection agency) and the *inspectee* (an aggregate representing all those whom it is the inspector's province to inspect). Goldman and Shier [3] have shown that in a non-cooperative game, with payoff functions satisfying an assumption obeyed by (2.4) below, such an aggregation of players into a single unit does not change the solution of the game.

*AMS subject classification: 90D40

[†]Center for Applied Mathematics, National Engineering Laboratory.

¹Figures in brackets indicate literature references at the end of this paper.

As in [2], the inspectee can either cheat, or not, for each of a set of devices, D_1, D_2, \dots, D_n . (These "devices" might be the measuring devices in n retail establishments, or the tax returns of n individuals.) The inspector selects some of these devices for inspection, up to the limit of his/her resources. The detection of a cheat, if the device is inspected, is assumed to be certain. We set:

- n = the number of devices available to the inspectee,
- V_i = the payoff to the inspectee from cheating on D_i ,
- P_i = the penalty imposed on the inspectee when cheating is detected on D_i ,
- m = the number of devices that the inspector can inspect.

We assume that $m < n$, and that all V_i and P_i are positive. It will be convenient to number the devices so that

$$P_1 \geq P_2 \geq P_3 \geq \dots \geq P_n. \tag{2.1}$$

A strategy for the inspectee is an n -component vector

$$\mathbf{c} = (c_1, c_2, \dots, c_n),$$

where c_i is the probability that the inspectee will cheat on D_i . A pure strategy for the inspector is the specification of a subset M of the set $N = \{1, 2, \dots, n\}$, where $i \in M$ denotes that D_i is inspected. Then, a (mixed) strategy for the inspector is a vector $\mathbf{p} = (p(M))$, where

$$p(M) = \text{Prob} [\{D_i : i \in M\} \text{ are the devices inspected}].$$

With each such \mathbf{p} we associate the quantities

$$\begin{aligned} p_i &= \text{Prob} [D_i \text{ is inspected}] \\ &= \sum \{p(M) : i \in M\}. \end{aligned}$$

Since c_i and p_i represent probabilities, we must have

$$0 \leq c_i \leq 1, \quad 0 \leq p_i \leq 1, \quad i = 1, 2, \dots, n. \tag{2.2}$$

There is no further restriction on \mathbf{c} . However, as was shown in [2], the limitation of the inspector's resources² (m) which prevents him/her from inspecting all of the devices (n) can be expressed as

$$\sum_{i=1}^n p_i = m. \tag{2.3}$$

The net expected payoff to the inspectee from device D_i is the expected gain from cheating minus the expected penalty, i.e.

$$V_i c_i - P_i (c_i p_i) = [V_i - P_i p_i] c_i.$$

Thus, the total net expected payoff to the inspectee when the two players choose strategies \mathbf{c} and \mathbf{p} respectively, is

$$F(\mathbf{c}, \mathbf{p}) = \sum_{i=1}^n [V_i - P_i p_i] c_i. \tag{2.4}$$

²The restriction that m be an integer is inherent in the definition of M . However, it is not essential in what follows. Equation (2.3), with any choice of m , $0 < m < n$, can be used to define the inspection resources available to the inspector.

From the “zero-sum” assumption that the interests of the two players are diametrically opposed, it follows that $-F(\mathbf{c}, \mathbf{p})$ is the expected payoff to the inspector. (Two of the three models in [2] involve alternatives to this assumption, but we shall retain it here.)

For each $i, i = 1, 2, \dots, n$, define q_i by

$$q_i = V_i/P_i. \tag{2.5}$$

Then the objective function (2.4) can be rewritten as

$$F(\mathbf{c}, \mathbf{p}) = \sum_{i=1}^n P_i (q_i - p_i) c_i. \tag{2.6}$$

As in [2], we set $N = \{1, 2, \dots, n\}$ and let

$$T = \{i : V_i > P_i\} = \{i : q_i > 1\},$$

$$\bar{T} = N - T = \{i : V_i \leq P_i\} = \{i : q_i \leq 1\}.$$

Thus, T represents the set of “tempting” devices, those on which the inspectee can profit from cheating even if the cheating is detected. For any subset S of N , we denote the number of members of S by $|S|$. Also, we set

$$P(S) = \sum_{i \in S} P_i, \quad q(S) = \sum_{i \in S} q_i,$$

$$V(S) = \sum_{i \in S} V_i, \quad p(S) = \sum_{i \in S} p_i,$$

etc.

The solution of the game which we have just described takes different forms according as

$$m \geq |T| + q(\bar{T}) \quad (\text{Case I}) \tag{2.7}$$

or its opposite

$$m < |T| + q(\bar{T}) \quad (\text{Case II}) \tag{2.8}$$

holds. These cases correspond roughly to adequate and inadequate inspection resources, respectively. Note that the adequacy of inspection resources is influenced by the size of the penalties as well as by m ; the larger the penalties, the smaller the term $q(\bar{T})$ in (2.7) and (2.8).

Cases I and II will be analyzed in sections 3 and 4, respectively. For illustration, section 5 applies the results to the situation in which penalties for detected cheating are proportional to gains from cheating, i.e., all q_i 's have the same value.

3. Case I

Here we assume that

$$m \geq |T| + q(\bar{T}) \quad (2.7)$$

which can also be expressed as

$$m \geq \sum_{i=1}^n \min(1, q_i). \quad (2.7a)$$

It will be convenient to set

$$\begin{aligned} U &= \{i : V_i < P_i\} = \{i : q_i < 1\} \\ W &= \{i : V_i = P_i\} = \{i : q_i = 1\} \end{aligned}$$

so that $\bar{T} = U \cup W$. Then (2.7a) becomes

$$m \geq |T \cup W| + q(U). \quad (2.7b)$$

THEOREM 1. (i) *The value of the game is*

$$F^\circ = V(T) - P(T).$$

(ii) *If \mathbf{p}° is a strategy for the inspector such that*

$$p_i^\circ \geq \min(1, q_i) \quad \text{for all } i$$

then \mathbf{p}° is optimal.

(iii) *If \mathbf{c}° is a strategy for the inspectee such that*

$$c_i^\circ = 1 \quad \text{for } i \in T$$

$$c_i^\circ = 0 \quad \text{for } i \in U$$

then \mathbf{c}° is optimal.

PROOF: First, set

$$p_i^\circ = 1 \quad \text{for } i \in T \cup W$$

From (2.3) and (2.7b) we have

$$q(U) \leq m - |T \cup W| = m - p^\circ(T \cup W) = p^\circ(U)$$

and

$$p^\circ(U) < n - |T \cup W| = |U|,$$

and hence the above settings can be extended to yield a strategy \mathbf{p}° for the inspector such that

$$p_i^\circ \geq q_i \quad \text{for } i \in U.$$

Thus the hypothesis of (ii) can be satisfied. Set $F^\circ = V(T) - P(T)$ and let \mathbf{c} be any strategy for the inspectee. It follows from (2.4) and (2.5) that

$$\begin{aligned} F^\circ - F(\mathbf{c}, \mathbf{p}^\circ) &= V(T) - P(T) - \sum_{i \in T \cup W} (V_i - P_i)c_i - \sum_{i \in U} (V_i - P_i p_i^\circ)c_i \\ &= \sum_{i \in T} (V_i - P_i)(1 - c_i) - \sum_{i \in U} P_i(q_i - p_i^\circ)c_i \\ &\geq 0. \end{aligned} \tag{3.1}$$

Now let \mathbf{c}° be any strategy for the inspectee satisfying the conditions of (iii). Then, for any strategy \mathbf{p} for the inspector,

$$\begin{aligned} F(\mathbf{c}^\circ, \mathbf{p}) - F^\circ &= \sum_{i \in T} (V_i - P_i p_i) - V(T) + P(T) + \sum_{i \in W} (V_i - P_i p_i)c_i^\circ \\ &= \sum_{i \in T} P_i(1 - p_i) + \sum_{i \in W} P_i(1 - p_i)c_i^\circ \\ &\geq 0. \end{aligned} \tag{3.2}$$

Combining equations (3.1) and (3.2), we have

$$F(\mathbf{c}^\circ, \mathbf{p}) \geq F^\circ \geq F(\mathbf{p}^\circ, \mathbf{c})$$

for all \mathbf{p} and for all \mathbf{c} . Hence the value of the game is F° , \mathbf{p}° is an optimal strategy for the inspector and \mathbf{c}° is an optimal strategy for the inspectee.

We now wish to determine whether or not there are any other optimal strategies. In Theorems 2 and 3 we will show that when $m > |T \cup W| + q(U)$ then no other optimal strategies exist for either player. However, when $m = |T \cup W| + q(U)$ then another class of optimal strategies for the inspectee exists.

THEOREM 2. *The strategy \mathbf{p}° for the inspector is optimal if and only if*

$$p_i^\circ \geq \min(1, q_i)$$

for all i .

PROOF. Let \mathbf{p}° be an optimal strategy for the inspector. It follows from eq (3.2) that if there exists $j \in T$ such that $p_j^\circ < 1$, then

$$F(\mathbf{c}^\circ, \mathbf{p}^\circ) - F^\circ \geq (1 - p_j^\circ) P_j > 0,$$

where \mathbf{c}° is the strategy defined in (iii) of Theorem 1. Hence \mathbf{p}° is not optimal. This is a contradiction and so

$$p_j^\circ = 1 \quad \text{for all } j \in T.$$

Similarly, if there exists $j \in W$ such that $p_j^\circ < 1$, then

$$F(\mathbf{c}^\circ, \mathbf{p}^\circ) - F^\circ \geq (1 - p_j^\circ) P_j c_j^\circ > 0$$

(for any choice of $c_j^\circ > 0$). Again, \mathbf{p}° is not optimal. This is a contradiction and thus we have shown that

$$p_j^\circ = 1 \quad \text{for all } j \in W.$$

It remains to show that

$$p_i^\circ \geq q_i \quad \text{for all } i \in U.$$

Suppose there exists $j \in U$ such that

$$p_j^\circ < q_j.$$

Consider a strategy $\tilde{\mathbf{c}}$ for the inspectee for which:

$$\begin{aligned} \tilde{c}_i &= 1 & \text{for all } i \in T, \\ \tilde{c}_j &= 1, \\ \tilde{c}_i &= 0, & \text{for } i \neq j, i \in U. \end{aligned}$$

Then

$$F(\mathbf{c}, \mathbf{p}^\circ) - F^\circ = (q_j - p_j^\circ) P_j > 0.$$

Thus \mathbf{p}° is not optimal. This is a contradiction and so we have shown that

$$p_j^\circ \geq q_j \quad \text{for all } j \in U.$$

Hence $p_i^\circ \geq \min(1, q_i)$ for all i .

The converse is part (ii) of Theorem 1.

We wish to show that if $m > |T \cup W| + q(U)$, then every optimal strategy for the inspectee is given by (iii) of Theorem 1. The proof of the following Lemma is trivial.

LEMMA 1. *If $m > |T \cup W| + q(U)$, then there exists a strategy \mathbf{p} for the inspector such that*

$$\begin{aligned} p_i &> q_i & i \in U \\ p_i &= 1 & i \in T \cup W \end{aligned}$$

THEOREM 3. *If $m > |T \cup W| + q(U)$, then \mathbf{c} is an optimal strategy for the inspectee if and only if*

$$\begin{aligned} c_i &= 1 & i \in T \\ c_i &= 0 & i \in U \end{aligned}$$

(so that c_i is arbitrary for $i \in W$).

PROOF. Let \mathbf{c}° be an optimal strategy for the inspectee and suppose that there exists $j \in T$ for which $c_j^\circ < 1$. By eq (3.1)

$$F^\circ - F(\mathbf{p}^\circ, \mathbf{c}^\circ) \geq (V_j - P_j)(1 - c_j^\circ) > 0,$$

where \mathbf{p}° is the strategy for the inspector define in Theorem 1. Hence \mathbf{c}° is not optimal. This is a contradiction and thus

$$c_j^\circ = 1 \quad \text{for all } j \in T.$$

Similarly, suppose that there exists $j \in U$ such that

$$c_j^\circ > 0.$$

Let \mathbf{p} be the strategy for the inspector described in the Lemma. By equation (3.1)

$$F^\circ - F(\mathbf{c}^\circ, \mathbf{p}) \geq - (q_j - p_j) P_j c_j^\circ > 0.$$

Hence \mathbf{c}° is not optimal. This is again a contradiction and so we have shown that

$$c_j^\circ = 0 \quad \text{for all } j \in U.$$

The converse follows from (iii) of Theorem 1.

The hypothesis that $m > |T \cup W| + q(U)$ of Theorem 3 was used only via Lemma 1, when showing that $c_j^\circ = 0$ for all $j \in U$. Hence, the following corollary is a consequence of the proof of Theorem 3 (whether $m > |T \cup W| + q(U)$ or not).

COROLLARY 1. If \mathbf{c}° is an optimal strategy for the inspectee then

$$c_i^\circ = 1 \quad \text{for all } i \in T.$$

In order to complete our consideration of Case I, it remains only to examine the situation where $m = |T \cup W| + q(U)$.

LEMMA 2. Let $m = |T \cup W| + q(U)$ and let \mathbf{c}° be an optimal strategy for the inspectee. For $h, j \in U$ we have

$$c_h^\circ P_h = c_j^\circ P_j.$$

PROOF. Suppose that for some $h, j \in U$, we have

$$c_h^\circ > \frac{c_j^\circ P_j}{P_h},$$

say

$$c_h^\circ - \frac{c_j^\circ P_j}{P_h} = a > 0.$$

Let $b = \min(q, 1 - q_h)$. Since $h, j \in U$, it follows that $b > 0$. Define the strategy $\tilde{\mathbf{p}}$ for the inspector by

$$\tilde{p}_h = q_h + b,$$

$$\tilde{p}_j = q_j - b,$$

$$\tilde{p}_i = \min(1, q_i) \quad i \neq h, j.$$

Note that $\tilde{\mathbf{p}}$ is a strategy vector since

$$\sum_{i=1}^n \tilde{p}_i = |T \cup W| + q(U) = m.$$

It follows from eq (2.4) and Corollary 1 that

$$\begin{aligned} F(\mathbf{c}^\circ, \tilde{\mathbf{p}}) - F^\circ &= \sum_{i \in T} (V_i - P_i)c_i^\circ - V(T) + P(T) + \sum_{i \in U} (V_i - P_i\tilde{p}_i)c_i^\circ \\ &= - \sum_{i \in T} (V_i - P_i)(1 - c_i^\circ) + [V_h - (q_h + b)P_h]c_h^\circ + [V_j - (q_j - b)P_j]c_j^\circ \\ &= [V_h - (q_h + b)P_h][c_j^\circ P_j/P_h + a] + [V_j - (q_j - b)P_j]c_j^\circ \\ &= -bP_jc_j^\circ - bP_ha + bP_jc_j^\circ \\ &= -bP_ha \\ &< 0. \end{aligned}$$

This is a contradiction of the optimality of \mathbf{c}° and hence we have shown that

$$c_h^\circ P_h = c_j^\circ P_j.$$

Let $m = |T \cup W| + q(U)$ and let \mathbf{c}° be an optimal strategy for the inspectee. Since $m < n$ it follows that U is not empty. By Lemma 2 there exists a number $M(\mathbf{c}^\circ)$ such that $M(\mathbf{c}^\circ) = c_h^\circ P_h$ for all $h \in U$.

LEMMA 3. Let $m = |T \cup W| + q(U)$ and let \mathbf{c}° be an optimal strategy for the inspectee. Then

$$c_i^\circ P_i \geq M(\mathbf{c}^\circ) \quad \text{for all } i \in W,$$

$$P_i \geq M(\mathbf{c}^\circ) \quad \text{for all } i \in T.$$

PROOF. Let $j \in U$ and suppose there exists $h \in W$ such that

$$c_h^\circ P_h < M(\mathbf{c}^\circ) = c_j^\circ P_j.$$

Define the strategy \tilde{p} for the inspector by

$$\begin{aligned}\tilde{p}_j &= 1, \\ \tilde{p}_h &= q_j, \\ \tilde{p}_i &= \min(1, q_i), \quad i \neq j, h.\end{aligned}$$

Then, using Corollary 1, we have

$$\begin{aligned}F(\mathbf{c}^\circ; \tilde{\mathbf{p}}) - F^\circ &= (1 - q_j)P_h c_h^\circ + (q_j - 1)P_j c_j^\circ + \sum_{i \in T} (V_i - P_i)(c_i^\circ - 1) \\ &= (1 - q_j)(P_h c_h^\circ - P_j c_j^\circ) \\ &< 0.\end{aligned}$$

This is a contradiction and hence

$$c_i^\circ P_i \geq M(\mathbf{c}^\circ) \quad \text{for all } i \in W$$

Now suppose that there exists $h \in T$ such that

$$P_h < M(\mathbf{c}^\circ) = c_j^\circ P_j$$

With \tilde{p} the strategy vector for the inspector as defined above, we have

$$\begin{aligned}F(\mathbf{c}^\circ; \tilde{\mathbf{p}}) - F^\circ &= (q_h - q_j)P_h c_h^\circ + (q_j - 1)P_j c_j^\circ - V_h + P_h + \sum_{\substack{i \in T \\ i \neq h}} (V_i - P_i)(c_i^\circ - 1) \\ &= (q_h - 1)P_h(c_h^\circ - 1) + (1 - q_j)[P_h c_h^\circ - M(\mathbf{c}^\circ)] \\ &< 0\end{aligned}$$

since $P_h c_h^\circ < P_h < M(\mathbf{c}^\circ)$. Again we have reached a contradiction and thus we have

$$P_i \geq M(\mathbf{c}^\circ) \quad \text{for all } i \in T.$$

We are now able to determine all of the optimal strategies \mathbf{c}° for the inspectee in the special case where $m = |T \cup W| + q(U)$.

THEOREM 4. *Let $m = |T \cup W| + q(U)$. A set of necessary and sufficient conditions in order that the strategy vector \mathbf{c}° be optimal for the inspectee are*

(i) *there exists a real number $M(\mathbf{c}^\circ)$ such that*

$$\begin{aligned}a) \quad c_i^\circ P_i &= M(\mathbf{c}^\circ) && \text{for all } i \in U, \\ b) \quad c_i^\circ P_i &\geq M(\mathbf{c}^\circ) && \text{for all } i \in W, \\ c) \quad P_i &\geq M(\mathbf{c}^\circ) && \text{for all } i \in T,\end{aligned}$$

$$(ii) \quad c_i^\circ = 1 \quad \text{for all } i \in T.$$

PROOF. The necessity of the conditions follows from Corollary 1, Lemma 2 and Lemma 3.

Now let \mathbf{c}° be a vector satisfying the conditions of the theorem. Then, for any strategy \mathbf{p} for the inspector,

$$\begin{aligned} F(\mathbf{c}^\circ, \mathbf{p}) - F^\circ &= \sum_{i \in T} (V_i - P_i p_i) - V(T) + P(T) + \sum_{i \in W} P_i (1 - p_i) c_i^\circ + \sum_{i \in U} (q_i - p_i) P_i c_i^\circ \\ &= \sum_{i \in T} P_i (1 - p_i) + \sum_{i \in W} P_i (1 - p_i) c_i^\circ + \sum_{i \in U} (q_i - p_i) M(\mathbf{c}^\circ). \end{aligned}$$

Set

$$c_i^\circ P_i - M(\mathbf{c}^\circ) = a_i \geq 0 \quad \text{for all } i \in W,$$

$$P_i - M(\mathbf{c}^\circ) = b_i \geq 0 \quad \text{for all } i \in T.$$

Then

$$\begin{aligned} F(\mathbf{c}^\circ, \mathbf{p}) - F^\circ &= \left[\sum_{i=1}^n \min(1, q_i) - \sum_{i=1}^n P_i \right] M(\mathbf{c}^\circ) + \sum_{i \in T} (1 - p_i) b_i + \sum_{i \in W} (1 - p_i) a_i \\ &= \sum_{i \in T} (1 - p_i) b_i + \sum_{i \in W} (1 - p_i) a_i \end{aligned}$$

since

$$\sum_{i=1}^n \min(1, q_i) = |T \cup W| + q(U) = m = \sum_{i=1}^n P_i.$$

Hence $F(\mathbf{c}^\circ, \mathbf{p}) - F^\circ \geq 0$ for all \mathbf{p} and so \mathbf{c}° is an optimal strategy for the inspectee.

COROLLARY 2. Let $m = |T \cup W| + q(U)$ and let M be a real number. A necessary and sufficient condition that there is an optimal strategy \mathbf{c}° for the inspectee such that $M(\mathbf{c}^\circ) = M$ is that

$$0 \leq M \leq \min_i P_i.$$

PROOF. Let \mathbf{c}° be an optimal strategy for the inspectee with $M(\mathbf{c}^\circ) = M$. Then

$$M = c_i^\circ P_i \leq P_i \quad \text{for all } i \in U,$$

$$M \leq c_i^\circ P_i \leq P_i \quad \text{for all } i \in W,$$

$$M \leq P_i \quad \text{for all } i \in T$$

and so $M \leq \min_i P_i$.

Conversely, let M be any number such that $0 \leq M \leq \min_i P_i$ and define c° by

$$c_i^\circ = 1 \quad \text{for all } i \in T \cup W,$$

$$c_i^\circ = M/P_i \quad \text{for all } i \in U.$$

Then c° is the desired optimal strategy for the inspectee.

This completes the case in which the inspector's resources are at least adequate for the job of inspecting the devices under his/her jurisdiction. The value of such a game is $F^\circ = V(T) - P(T)$, which is independent of m . The inspectee cannot, of course, be prevented from benefitting by cheating on the tempting devices (T), but he/she gains nothing (or actually decreases his/her expectation) by cheating on the other devices ($U \cup W$). When the inspector's resources are just barely adequate for his/her responsibilities (i.e. $m = |T \cup W| + q(U)$), the inspectee has a wider variety of optimal strategies to choose from (e.g., including cheating on the devices in $U \cup W$ with probabilities inversely proportional to the associated penalties) but the value of the game remains the same. We now turn to the case of inadequate inspection resources.

4. Case II

The defining relation for Case II, which describes the inspection resources as being below a certain adequacy threshold, is

$$m < |T \cup W| + q(U) = \sum_{i=1}^n \min(1, q_i). \quad (4.1)$$

Recall that in (2.1) we have numbered the devices so that

$$P_1 \geq P_2 \geq P_3 \geq \dots \geq P_n.$$

It follows from (4.1) that there exists an integer k , $0 \leq k < n$, such that

$$\sum_{i=1}^k \min(1, q_i) \leq m < \sum_{i=1}^{k+1} \min(1, q_i). \quad (4.2)$$

If the P_i 's are not distinct then the condition of (2.1) does not assign a number to each device in a unique manner. This ambiguity in numbering the devices may in turn affect the value of k as defined by (4.2). However, the subsequent material does not depend on which of the possible numberings obeying (4.2) is used. Once k has been determined, we set

$$G = \{i \mid P_i > P_{k+1}\} \quad ,$$

$$E = \{i \mid P_i = P_{k+1}\} \quad ,$$

$$L = \{i \mid P_i < P_{k+1}\} \quad .$$

Note that G , E and L are independent of which of the possible numberings of the devices obeying (2.1) has been used. Clearly E is not empty, although either G or L might be. Set $K = \{1, 2, \dots, k\}$ with the understanding that K is empty if $k=0$. Then

$$G \subseteq K \subset K \cup \{k+1\} \subseteq G \cup E$$

and so

$$\sum_{i \in G} \min(1, q_i) \leq \sum_{i=1}^k \min(1, q_i) \leq m < \sum_{i=1}^{k+1} \min(1, q_i) \leq \sum_{i \in G \cup E} \min(1, q_i).$$

Then, setting

$$\begin{aligned} g &= m - \sum_{i \in G} \min(1, q_i) \\ &= m - |G \cap T| - q(G \cap \bar{T}), \end{aligned} \quad (4.3)$$

we have

$$0 \leq g < \sum_{i \in E} \min(1, q_i). \quad (4.4)$$

We will show that

$$F^\circ = V(G \cap T) + V(E) + V(L) - P_{k+1}g - P(G \cap T) \quad (4.5)$$

is the value of the game.

LEMMA 4. Let F° be defined as in (4.5) and let \mathbf{p}° be any strategy for the inspector which satisfies

$$\begin{aligned} (i) \quad p_i^\circ &= \min(1, q_i) && \text{for all } i \in G, \\ (ii) \quad p_i^\circ &= 0 && \text{for all } i \in L, \\ (iii) \quad p_i^\circ &\leq \min(1, q_i) && \text{for all } i \in E. \end{aligned}$$

Then $F^\circ \geq F(\mathbf{c}, \mathbf{p}^\circ)$ for all strategies \mathbf{c} for the inspectee.

PROOF. It follows as a consequence of (i), (ii) and (4.3) that

$$(iv) \quad p^\circ(E) = g.$$

Substituting (i) and (ii) into (2.4), we have

$$F(\mathbf{c}, \mathbf{p}^\circ) = \sum_{i \in G \cap T} (V_i - P_i)c_i + \sum_{i \in G \cap \bar{T}} (V_i - P_i q_i)c_i + \sum_{i \in E} (V_i - P_{k+1} p_i^\circ)c_i + \sum_{i \in L} V_i c_i.$$

But $V_i - P_i q_i = 0$ for all $i \in G \cap \bar{T}$. It follows from (4.5) and (iv) that

$$F^\circ - F(\mathbf{c}, \mathbf{p}^\circ) = \sum_{i \in G \cap T} P_i(q_i - 1)(1 - c_i) + \sum_{i \in E} (V_i - P_{k+1} p_i^\circ)(1 - c_i) + \sum_{i \in L} V_i(1 - c_i). \quad (4.6)$$

However, $q_i - 1 > 0$ for $i \in G \cap T$ and, by (iii),

$$V_i - P_{k+1} p_i^\circ \geq 0 \quad \text{for all } i \in E.$$

Hence each term on the right hand side of the last equation is non-negative and so

$$F^\circ - F(\mathbf{c}, \mathbf{p}^\circ) \geq 0$$

for all strategies \mathbf{c} for the inspectee.

COROLLARY 3. Let $\tilde{\mathbf{c}}$ be a strategy for the inspectee. In order that $F(\tilde{\mathbf{c}}, \mathbf{p}) = F^\circ$ for all strategies \mathbf{p} for the inspector which satisfy conditions (i) through (iv) of the lemma, it is necessary and sufficient that

$$\begin{aligned} \text{(v)} \quad \tilde{c}_i &= 1 && \text{for all } i \in G \cap T, \\ \text{(vi)} \quad \tilde{c}_i &= 1 && \text{for all } i \in L, \\ \text{(vii)} \quad \tilde{c}_i &= 1 && \text{for all } i \in E. \end{aligned}$$

PROOF. It follows immediately from (4.6) that conditions (v) through (vii) form a set of sufficient conditions that $F(\tilde{\mathbf{c}}, \mathbf{p}) = F^\circ$ for all strategies \mathbf{p} which satisfy conditions (i) through (iv).

Since $q_i - 1 > 0$ for all $i \in G \cap T$ and $V_i > 0$ for all $i \in L$, (4.6) also shows that (v) and (vi) are necessary conditions that $F(\tilde{\mathbf{c}}, \mathbf{p}) = F^\circ$ for all strategies \mathbf{p} satisfying (i) through (iv). It remains to show that condition (vii) is also necessary. By (4.4), for each $j \in E$ there exists a strategy for the inspector, \mathbf{p}^j , satisfying (i) through (iv) and such that

$$p_j^j < \min(1, q_j).$$

Then

$$V_j - P_{k+1} p_j^j > 0.$$

By (4.6), in order that $F(\tilde{\mathbf{c}}, \mathbf{p}^j) = F^\circ$, it is necessary that $\tilde{c}_j = 1$. Hence we have shown that condition (vii) is also necessary.

LEMMA 5. If $\tilde{\mathbf{c}}$ is any strategy for the inspectee which satisfies conditions (v) through (vii) of Corollary 3 then

$$F(\tilde{\mathbf{c}}, \mathbf{p}) - F^\circ = \sum_{i \in G \cap T} (P_i - P_{k+1})(1 - p_i) + \sum_{i \in L} (P_{k+1} - P_i)p_i + \sum_{i \in G \cap \bar{T}} (P_i \tilde{c}_i - P_{k+1})(q_i - p_i) \quad (4.7)$$

for all \mathbf{p} . If $\bar{\mathbf{c}}$ is any strategy for the inspectee which satisfies conditions (v) through (vii) and, in addition, satisfies

$$\text{(viii)} \quad \bar{c}_i = P_{k+1}/P_i \quad \text{for all } i \in G \cap U$$

then

$$F(\bar{\mathbf{c}}, \mathbf{p}) - F^\circ = \sum_{i \in G \cap T} (P_i - P_{k+1})(1 - p_i) + \sum_{i \in L} (P_{k+1} - P_i)p_i + \sum_{i \in G \cap W} (P_i \bar{c}_i - P_{k+1})(1 - p_i) \quad (4.8)$$

for all \mathbf{p} .

PROOF. Let $\tilde{\mathbf{c}}$ be a strategy for the inspectee which satisfies (v) through (vii). Substituting (v) through (vi) into (2.4), we have

$$\begin{aligned} F(\tilde{\mathbf{c}}, \mathbf{p}) &= \sum_{i \in G \cap T} (V_i - P_i p_i) + \sum_{i \in G \cap \bar{T}} P_i (q_i - p_i) \tilde{c}_i + \sum_{i \in E} (V_i - P_{k+1} p_i) + \sum_{i \in L} (V_i - P_i p_i) \\ &= V(G \cap T) + V(E) + V(L) + P_{k+1} [q(G \cap \bar{T}) - p(G \cap \bar{T}) - p(E)] \\ &\quad - \sum_{i \in G} P_i p_i - \sum_{i \in L} P_i p_i + \sum_{i \in G \cap \bar{T}} (P_i \tilde{c}_i - P_{k+1})(q_i - p_i). \end{aligned}$$

It follows from (4.5) that

$$F(\mathbf{c}, \mathbf{p}) - F^\circ = P_{k+1}[q(G \cap \bar{T}) - p(G \cap \bar{T}) - p(E) + g] - \sum_{i \in L} P_i p_i \\ + \sum_{i \in G \cap \bar{T}} (P_i \bar{c}_i - P_{k+1})(q_i - p_i) + \sum_{i \in G \cap T} P_i (1 - p_i).$$

Solving eq (4.3) for m , we have

$$m = g + |G \cap T| + q(G \cap \bar{T})$$

and so the last equation becomes

$$F(\mathbf{c}, \mathbf{p}) - F^\circ = P_{k+1}[m - p(G \cap T) - p(G \cap \bar{T}) - p(E) - p(L)] + \sum_{i \in L} (P_{k+1} - P_i)p_i \\ + \sum_{i \in G \cap T} (P_i - P_{k+1})(1 - p_i) + \sum_{i \in G \cap \bar{T}} (P_i \bar{c}_i - P_{k+1})(q_i - p_i).$$

By eq (2.3),

$$m = p(G \cap T) + p(G \cap \bar{T}) + p(E) + p(L)$$

and consequently we are left with

$$F(\mathbf{c}, \mathbf{p}) - F^\circ = \sum_{i \in L} (P_{k+1} - P_i)p_i + \sum_{i \in G \cap T} (P_i - P_{k+1})(1 - p_i) + \sum_{i \in G \cap \bar{T}} (P_i \bar{c}_i - P_{k+1})(q_i - p_i)$$

which is eq (4.7).

If $\bar{\mathbf{c}}$ is a strategy for the inspectee which satisfies condition (viii) then

$$P_i \bar{c}_i - P_{k+1} = 0 \quad \text{for all } i \in G \cap U.$$

Thus, if $\bar{\mathbf{c}}$ satisfies conditions (v) through (viii) then eq (4.7) becomes (4.8).

It follows from equation (4.8) that:

COROLLARY 4. If \mathbf{c}° is a strategy for the inspectee which satisfies conditions (v) through (viii) and also satisfies

$$(ix) \ c_i^\circ \geq P_{k+1}/P_i \quad \text{for all } i \in G \cap W,$$

then $F(\mathbf{c}^\circ, \mathbf{p}) \geq F^\circ$ for all \mathbf{p} .

We can now describe the solution of the game in Case II.

THEOREM 5. (a) The value of the game is F° . (b) If \mathbf{p}° is a strategy for the inspector which satisfies (i) through (iv) then \mathbf{p}° is optimal. (c) If \mathbf{c}° is a strategy for the inspectee which satisfies (v) through (ix) then \mathbf{c}° is optimal.

PROOF. First we wish to show that there exist strategies \mathbf{p}° and \mathbf{c}° which satisfy conditions (i) through (iii) and (v) through (ix) respectively. It is readily verified that if \mathbf{p}° is defined by

$$\begin{aligned} p_i^\circ &= \min(1, q_i) && \text{for all } i \in G, \\ p_i^\circ &= 0 && \text{for all } i \in L, \\ p_i^\circ &= g \min(1, q_i) / \left\{ \sum_{j \in E} \min(1, q_j) \right\} && \text{for all } i \in E \end{aligned}$$

then \mathbf{p}° is a strategy for the inspector and \mathbf{p}° satisfies (i) through (iv).

Similarly, if \mathbf{c}° is defined by

$$\begin{aligned} c_i^\circ &= 1 && \text{for all } i \in G \cap T, \\ c_i^\circ &= 1 && \text{for all } i \in L, \\ c_i^\circ &= 1 && \text{for all } i \in E, \\ c_i^\circ &= P_{k+1}/P_i && \text{for all } i \in G \cap \bar{T}, \end{aligned}$$

then \mathbf{c}° is a strategy for the inspectee and \mathbf{c}° satisfies (v) through (ix).

The Theorem now follows from Lemma 4 and Corollary 4.

Theorem 5 provides sets of sufficient conditions for strategies of each of the players to be optimal. In Theorem 6 we will show that the converse of part (b) of Theorem 5 holds, that is, conditions (i) through (iv) are both necessary and sufficient for a strategy for the inspector to be optimal. However, conditions (v) through (ix) are not necessary for a strategy for the inspectee to be optimal. In Theorems 7 and 8 we will provide a set of necessary and sufficient conditions that a strategy for the inspectee be optimal.

COROLLARY 5. If \mathbf{c}° is an optimal strategy for the inspectee then \mathbf{c}° satisfies conditions (v) through (vii).

PROOF. Let \mathbf{c}° be an optimal strategy for the inspectee and let \mathbf{p} be any strategy for the inspector which satisfies conditions (i) through (iv). By Theorem 5 (b), \mathbf{p} is an optimal strategy for the inspector. By Theorem 5 (a), $F(\mathbf{c}^\circ, \mathbf{p}) = F^\circ$ and by Corollary 3, \mathbf{c}° satisfies conditions (v) through (vii).

We can now identify all of the optimal strategies for the inspector.

THEOREM 6. The strategy \mathbf{p}° for the inspector is optimal if and only if \mathbf{p}° satisfies conditions (i) through (iv).

PROOF. By Theorem 5 (b), a strategy \mathbf{p}° for the inspector which satisfies conditions (i) through (iv) is optimal. Conversely, let \mathbf{p}° be an optimal strategy for the inspector and let \mathbf{c}° be a strategy for the inspectee which satisfies conditions (v) through (viii) and also

$$(x) \quad c_i^\circ = P_{k+1}/P_i \quad \text{for all } i \in G \cap \bar{W}.$$

Since condition (x) is stronger than condition (ix), it follows from Theorem 5 (c) that \mathbf{c}° is optimal. It then follows from Theorem 5 (a) that $F(\mathbf{c}^\circ, \mathbf{p}^\circ) = F^\circ$. Consequently, eq (4.8) becomes

$$0 = \sum_{i \in G \cap T} (P_i - P_{k+1})(1 - p_i^\circ) + \sum_{i \in L} (P_{k+1} - P_i)p_i^\circ.$$

But

$$\begin{aligned} P_i - P_{k+1} &> 0 && \text{for all } i \in G \cap T, \\ P_{k+1} - P_i &> 0 && \text{for all } i \in L. \end{aligned} \tag{4.9}$$

Thus, we must have

$$\begin{aligned} p_i^\circ &= 1 && \text{for all } i \in G \cap T \\ p_i^\circ &= 0 && \text{for all } i \in L. \end{aligned} \tag{4.10}$$

Now, for each $h \in G \cap \bar{T}$ we define two strategies for the inspectee, \mathbf{c}^h and $\bar{\mathbf{c}}^h$, as follows:

$\tilde{\mathbf{c}}^h$ and $\bar{\mathbf{c}}^h$ satisfy conditions (v) through (vii)

$$\begin{aligned}\tilde{c}_i^h &= \bar{c}_i^h = P_{k+1}/P_i & \text{for all } i \in G \cap \bar{T}, i \neq h \\ \tilde{c}_h^h &= 1, & \bar{c}_h^h &= 0.\end{aligned}$$

Since \mathbf{p}° is an optimal strategy for the inspector we have

$$\begin{aligned}F^\circ - F(\tilde{\mathbf{c}}^h, \mathbf{p}^\circ) &\geq 0, \\ F^\circ - F(\bar{\mathbf{c}}^h, \mathbf{p}^\circ) &\geq 0.\end{aligned}$$

Since $\tilde{\mathbf{c}}^h$ and $\bar{\mathbf{c}}^h$ satisfy conditions (v) through (vii), we may apply Lemma 5. Substituting eq (4.9) and (4.10) into eq (4.7), we have

$$\begin{aligned}F^\circ - F(\tilde{\mathbf{c}}^h, \mathbf{p}^\circ) &= (P_h - P_{k+1})(q_h - p_h^\circ) \geq 0, \\ F^\circ - F(\bar{\mathbf{c}}^h, \mathbf{p}^\circ) &= (-P_{k+1})(q_h - p_h^\circ) \geq 0,\end{aligned}$$

from which it follows that

$$p_h^\circ = q_h \quad \text{for all } h \in G \cap \bar{T}.$$

We have now shown that \mathbf{p}° satisfies conditions (i) and (ii) and consequently, as in Lemma 4, we have

$$p^\circ(E) = g.$$

It remains only to prove that \mathbf{p}° satisfies condition (iii).

Suppose that there exists $r \in E$ for which $p_r^\circ > q_r$. We define the strategy \mathbf{c}' for the inspectee by

$$\begin{aligned}\mathbf{c}' \text{ satisfies conditions (v), (vi) and (viii),} \\ c'_i &= 1 & \text{for all } i \in E, i \neq r, \\ c'_r &= 0,\end{aligned}$$

that is, \mathbf{c}' differs from the strategy $\bar{\mathbf{c}}$ of Lemma 5 for the inspectee only in that $c'_r=0$ whereas $\bar{c}_r=1$. By a computation similar to that of Lemma 5, we find

$$\begin{aligned}F(\mathbf{c}', \mathbf{p}^\circ) - F^\circ &= \sum_{\substack{i \in E \\ i \neq r}} P_{k+1}(q_i - p_i^\circ) - V(E) + gP_{k+1} \\ &= \sum_{i \in E} P_{k+1}(q_i - p_i^\circ) - V(E) + gP_{k+1} - P_{k+1}(q_r - p_r^\circ) \\ &= -P_{k+1}(q_r - p_r^\circ) > 0.\end{aligned}$$

However, since \mathbf{p}° is an optimal strategy, we must have

$$F(\mathbf{c}', \mathbf{p}^\circ) - F^\circ < 0.$$

This is a contradiction and so we have shown that

$$q_i \geq p_i^\circ \quad \text{for all } i \in E,$$

which proves that \mathbf{p}° satisfies condition (iii).

It remains to find a set of necessary and sufficient conditions that a strategy for the inspectee be optimal.

LEMMA 6. *If \mathbf{c}° is an optimal strategy for the inspectee then \mathbf{c}° satisfies*

$$(xi) \ c_i^\circ \geq P_{k+1}/P_i \quad \text{for all } i \in G \cap \bar{T}.$$

PROOF. For $j \in E$, let \mathbf{p}^j be the optimal strategy for the inspector defined in Corollary 3, that is, \mathbf{p}^j satisfies conditions (i) through (iv) and

$$p_j^j < \min(1, q_j).$$

Consider any $h \in G \cap \bar{T}$; it follows from condition (i) that

$$p_h^j = q_h.$$

We choose any u such that

$$0 < u < \min(q_h, 1 - p_j^j)$$

and define the (not optimal) strategy $\tilde{\mathbf{p}}$ by

$$\begin{aligned} \tilde{p}_j &= p_j^j + u, \\ \tilde{p}_h &= p_h^j - u = q_h - u, \\ \tilde{p}_i &= p_i^j \quad \text{for all } i, i \neq j, h. \end{aligned}$$

Since \mathbf{c}° is an optimal strategy,

$$F(\mathbf{c}^\circ, \tilde{\mathbf{p}}) - F^\circ \geq 0$$

and, by Corollary 5, \mathbf{c}° satisfies conditions (v) through (vii). By eq (4.7),

$$\begin{aligned} F(\mathbf{c}^\circ, \tilde{\mathbf{p}}) - F^\circ &= \sum_{i \in G \cap \bar{T}} (P_i c_i^\circ - P_{k+1})(q_i - \tilde{p}_i) \\ &= (P_k c_h^\circ - P_{k+1})u. \end{aligned}$$

Thus $P_h c_h^\circ - P_{k+1} \geq 0$, that is,

$$c_h^\circ \geq P_{k+1}/P_h,$$

and so \mathbf{c}° satisfies condition (xi).

LEMMA 7. *If \mathbf{c}° is an optimal strategy for the inspectee then there exists a real number $M(\mathbf{c}^\circ) \geq 0$ such that*

$$(xii) \quad P_i c_i^\circ - P_{k+1} = M(\mathbf{c}^\circ) \quad \text{for all } i \in G \cap U,$$

$$(xiii) \quad P_i c_i^\circ - P_{k+1} \geq M(\mathbf{c}^\circ) \quad \text{for all } i \in G \cap W.$$

PROOF. If $G \cap U$ is empty then, by Lemma 6, 0 will do for $M(\mathbf{c}^\circ)$. Hence we assume that there exists $j \in G \cap U$ and consider any $h \in G \cap \bar{T}, j \neq h$. Choose u such that

$$0 < u < \min(q_h, 1 - q_j).$$

Let \mathbf{p}° be an optimal strategy for the inspector and define $\tilde{\mathbf{p}}$ by

$$\tilde{p}_h = q_h - u,$$

$$\tilde{p}_j = q_j + u,$$

$$\tilde{p}_i = p_i^\circ \quad \text{for all } i, i \neq j, h.$$

By eq (4.7), we have

$$F(\mathbf{c}^\circ, \tilde{\mathbf{p}}) - F^\circ = (P_j c_j^\circ - P_{k+1})(-u) + (P_h c_h^\circ - P_{k+1})u.$$

Since \mathbf{c}° is an optimal strategy,

$$F(\mathbf{c}^\circ, \tilde{\mathbf{p}}) - F^\circ \geq 0.$$

Hence

$$P_h c_h^\circ - P_{k+1} \geq P_j c_j^\circ - P_{k+1}.$$

We set

$$P_j c_j^\circ - P_{k+1} = M(\mathbf{c}^\circ).$$

Thus we have shown that

$$P_i c_i^\circ - P_{k+1} \geq M(\mathbf{c}^\circ) \quad \text{for all } i \in G \cap \bar{T}.$$

If h (as well as j) belongs to $G \cap U$ then this argument can be repeated with j and h interchanged. Thus

$$P_h c_h^\circ - P_{k+1} = P_j c_j^\circ - P_{k+1} = M(\mathbf{c}^\circ) \quad \text{for all } h, j \in G \cap U.$$

By Lemma 6, $M(\mathbf{c}^\circ) \geq 0$.

LEMMA 8. Let \mathbf{c}° be an optimal strategy for the inspectee. If $g > 0$ and $G \cap U$ is not empty then $M(\mathbf{c}^\circ) = 0$, that is, \mathbf{c}° satisfies condition (viii), namely,

$$(viii) \quad c_i^\circ = P_{k+1}/P_i \quad \text{for all } i \in G \cap U.$$

PROOF. Since $G \cap U$ is not empty, we may select $j \in G \cap U$. Let \mathbf{p}° be an optimal strategy for the inspector. Since $g > 0$, (iv) shows that there exists $h \in E$ such that

$$p_h^\circ > 0.$$

Choose a real number u such that

$$0 < u < \min(p_h^\circ, 1 - q_j)$$

and define the strategy $\tilde{\mathbf{p}}$ for the inspector by

$$\begin{aligned} \tilde{p}_h &= p_h^\circ - u, \\ \tilde{p}_j &= p_j^\circ + u = q_j + u, \\ \tilde{p}_i &= p_i^\circ \quad \text{for all } i, i \neq h, j. \end{aligned}$$

Then a simple calculation yields

$$F(\mathbf{c}^\circ, \tilde{\mathbf{p}}) - F^\circ = -uP_j c_j^\circ + uP_{k+1}.$$

Since $j \in G \cap U$, it follows from Lemma 7 that

$$F(\mathbf{c}^\circ, \tilde{\mathbf{p}}) - F^\circ = -uM(\mathbf{c}^\circ).$$

However, \mathbf{c}° is optimal and thus

$$F(\mathbf{c}^\circ, \tilde{\mathbf{p}}) - F^\circ \geq 0.$$

By Lemma 6, $M(\mathbf{c}^\circ) \geq 0$ and so we have $M(\mathbf{c}^\circ) = 0$, which is equivalent to condition (viii).

We are now able to identify all of the optimal strategies for the inspectee. Theorem 7 will show that if $G \cap U$ is empty or if $g > 0$, then the optimal strategies are those described in (c) of Theorem 5. However, when both of these conditions are violated then there is an additional class of optimal strategies. These will be described in Theorem 8.

THEOREM 7. If either $G \cap U$ is empty or $g > 0$ then \mathbf{c}° is an optimal strategy for the inspectee if and only if \mathbf{c}° satisfies conditions (v) through (ix).

PROOF. Let \mathbf{c}° be an optimal strategy for the inspectee. By Corollary 5, \mathbf{c}° satisfies conditions (v) through (vii). If $G \cap U$ is empty then condition (viii) is satisfied vacuously. If $g > 0$ and $G \cap U$ is not empty then, by Lemma 8, condition (viii) is satisfied. Finally, by Lemma 6, condition (ix) is satisfied.

The converse is (c) of Theorem 5.

THEOREM 8. Let $g = 0$ and let $G \cap U$ not be empty. Then \mathbf{c}° is an optimal strategy for the inspectee if and only if \mathbf{c}° satisfies conditions (v) through (vii) and there exists a real number $M(\mathbf{c}^\circ)$,

$$0 \leq M(\mathbf{c}^\circ) \leq \min_{i \in G} P_i - P_{k+1}, \quad (4.11)$$

such that \mathbf{c}° satisfies

$$\begin{aligned} (xii) \quad & P_i c_i^\circ - P_{k+1} = M(\mathbf{c}^\circ) \quad \text{for all } i \in G \cap U, \\ (xiii) \quad & P_i c_i^\circ - P_{k+1} \geq M(\mathbf{c}^\circ) \quad \text{for all } i \in G \cap U. \end{aligned}$$

PROOF. Let \mathbf{c}° be a strategy for the inspectee which satisfies conditions (v), (vi), (vii), (xii) and (xiii), where $M(\mathbf{c}^\circ)$ be a real number satisfying (4.11). By Lemma 5,

$$F(\mathbf{c}^\circ, \mathbf{p}) - F^\circ = \sum_{i \in G \cap T} (P_i - P_{k+1})(1 - p_i) + \sum_{i \in L} (P_{k+1} - P_i)p_i + \sum_{i \in G \cap \bar{T}} (P_i c_i^\circ - P_{k+1})(q_i - p_i) \quad (4.12)$$

for any strategy \mathbf{p} for the inspector. For each $i \in G \cap T$, set

$$P_i c_i^\circ - P_{k+1} - M(\mathbf{c}^\circ) = a_i \geq 0.$$

Then eq (4.12) becomes

$$\begin{aligned} F(\mathbf{c}^\circ, \mathbf{p}) - F^\circ = & \sum_{i \in G \cap T} (P_i - P_{k+1})(1 - p_i) + \sum_{i \in L} (P_{k+1} - P_i)p_i \\ & + \sum_{i \in G \cap U} (M(\mathbf{c}^\circ)(q_i - p_i) + \sum_{i \in G \cap W} [M(\mathbf{c}^\circ) + a_i](1 - p_i). \end{aligned} \quad (4.13)$$

Since $g=0$, it follows from eq (4.3) that

$$\begin{aligned} m &= |G \cap T| + q(G \cap \bar{T}) \\ &= p(G \cap T) + p(G \cap \bar{T}) + p(E) + p(L). \end{aligned}$$

Thus,

$$q(G \cap \bar{T}) - p(G \cap \bar{T}) = p(G \cap T) + p(E) + p(L) - |G \cap T|. \quad (4.14)$$

Substituting eq (4.14) into eq (4.13) yields

$$\begin{aligned} F(\mathbf{c}^\circ, \mathbf{p}) - F^\circ &= \sum_{i \in G \cap T} (P_i - P_{k+1})(1 - p_i) + \sum_{i \in L} (P_{k+1} - P_i)p_i \\ &+ M(\mathbf{c}^\circ)[p(G \cap T) + p(E) + p(L) - |G \cap T|] + \sum_{i \in G \cap W} a_i(1 - p_i) \\ &= \sum_{i \in G \cap T} [P_i - P_{k+1} - M(\mathbf{c}^\circ)](1 - p_i) + \sum_{i \in L} [P_{k+1} - P_i + M(\mathbf{c}^\circ)] p_i + \sum_{i \in E} M(\mathbf{c}^\circ)p_i \\ &+ \sum_{i \in G \cap W} a_i(1 - p_i) \geq 0 \end{aligned}$$

for all strategies \mathbf{p} for the inspector, since $P_i - P_{k+1} - M(\mathbf{c}^\circ) \geq 0$ for all $i \in G \cap T$. Thus we have shown that \mathbf{c}° is an optimal strategy.

Conversely, let \mathbf{c}° be an optimal strategy for the inspectee. By Corollary 5 and Lemma 7, \mathbf{c}° satisfies conditions (v), (vi), (vii), (xii) and (xiii) for some $M(\mathbf{c}^\circ) \geq 0$. It remains only to show that $M(\mathbf{c}^\circ)$ satisfies the right-hand inequality in (4.11). Suppose it does not. Then there exists $h \in G \cap T$ such that

$$M(\mathbf{c}^\circ) > P_h - P_{k+1},$$

that is,

$$P_h - P_{k+1} - M(\mathbf{c}^\circ) < 0.$$

Since $G \cap U$ is not empty, there exists $j \in G \cap U$ and so $q_j < 1$. Define the strategy \mathbf{p} for the inspector by

$$\begin{aligned} p_h &= q_j \\ p_j &= 1 \\ p_i &= 1 && \text{for all } i \in G \cap T, i \neq h, \\ p_i &= q_i && \text{for all } i \in G \cap \bar{T}, i \neq j, \\ p_i &= 0 && \text{for all } i \in E \cap L. \end{aligned}$$

Then

$$F(\mathbf{c}^\circ, \mathbf{p}) - F^\circ = [P_h - P_{h+1} - M(\mathbf{c}^\circ)](1 - q_j) < 0,$$

which contradicts the fact that \mathbf{c}° is an optimal strategy for the inspectee. Hence $M(\mathbf{c}^\circ)$ satisfies (4.11).

Table of Results

| Case Definition | Inspectee's Strategy | Inspector's Strategy | Payoff |
|--|--|--|--|
| Case I $m > T + q(\bar{T})$ $m = T + q(\bar{T})$ | $p_i^\circ \geq \min(1, q_j)$ | $c_i^\circ = 1 \quad i \in T$ $c_i^\circ = 0 \quad i \in U$ | $F^\circ = V(T) - P(T)$ |
| | $p_i^\circ = \min(1, q_j)$ | $c_i^\circ P_i = M(\mathbf{c}^\circ) \quad i \in U$ $c_i^\circ P_i > M(\mathbf{c}^\circ) \quad i \in W$ $c_i^\circ = 1 \quad i \in T$ | $F^\circ = V(T) - P(T)$ |
| Case II $m < T + q(\bar{T})$ | $p_i^\circ = \min(1, q_j) \quad i \in G$ $p_i^\circ = 0 \quad i \in L$ $p_i^\circ < \min(1, q_j) \quad i \in E$ $\mathbf{p}^\circ(E) = g$ | $c_i^\circ = 1 \quad i \in G \cap T$ $c_i^\circ = 1 \quad i \in L$ $c_i^\circ = 1 \quad i \in E$ $c_i^\circ = P_{i+1}/P_i \quad i \in G \cap U$ $c_i^\circ > P_{i+1}/P_i \quad i \in G \cap W$ for $G \cap U = \emptyset$ or $g > 0$ $c_i^\circ = 1 \quad i \in G \cap T$ $c_i^\circ = 1 \quad i \in L$ $c_i^\circ = 1 \quad i \in E$ $c_i^\circ P_i - P_{i+1} = M(\mathbf{c}^\circ) \quad i \in G \cap U$ $c_i^\circ P_i - P_{i+1} > M(\mathbf{c}^\circ) \quad i \in G \cap W$ for $G \cap U \neq \emptyset$ and $g = 0$ | $F^\circ = V(G \cap T) + V(E) + V(L) - P_{i+1}g - P(G \cap T)$ |

5. Example: Proportional Penalties

Our aim in this section is to illustrate the preceding material by applying it to some simple situation. Three possibilities suggest themselves for this illustrative role. One is the situation in which all penalties P_i have a common value P . This, however, is precisely Model 1 of our previous paper [2], and so it need not be repeated here. The other two "scenarios" are both natural generalizations of Example 1: *Equal-Sized Firms* given in section 3 of [2]. One of them involves a common value V for the cheating-gains V_i ; the other postulates a common value q for all the quotients $q_i = V_i/P_i$. The latter situation, in which penalties for detected cheating are proportional to gains from cheating, leads to results which are simpler and more readily interpretable and it is also more relevant in the (income-tax return audit) context of [1]. This constant- q situation was therefore selected for presentation below.

Suppose first that $q > 1$. Then all n devices are "tempting", i.e., $T = N$, while \bar{T} , U and W are empty. The right-hand side of (2.7) and (2.8) reduce to n . Since $m < n$, Case II is governing. It follows from (4.2) that k is the greatest integer not exceeding m , which we denote $k = [m]$. From (4.3), we have $g = m - |G|$.

The value of the game, according to (4.5) and (a) of Theorem 5, is given by

$$\begin{aligned} F^\circ &= V(G) - P(G) + V(E \cup L) - P_{k+1}g \\ &= (q-1)P(G) + q[P(N) - P(G)] - P_{k+1}(m - |G|) \\ &= qP(N) - mP_{k+1} - [P(G) - P_{k+1}|G|]. \end{aligned} \tag{5.1}$$

It is interesting to think of the P_i 's as fixed and to see how F° , a measure of the (mis)performance of the inspection system, varies with m (a measure of the inspection-resources available) and q (a measure of the incentive to cheat). For each integer k , with $0 \leq k \leq n-1$, it follows from (5.1) that F° is linear in q and m in the vertical strip $\{(m, q): k \leq m < k+1, q > 1\}$ of the (m, q) -plane; as would be expected, F° increases with q and decreases with m .

The optimal strategies \mathbf{p}° for the inspector are given by (b) of Theorem 5: one should always inspect those devices with penalties greater than the critical level P_{k+1} , never inspect those with penalties below this level, and allocate the balance (if any) of his/her effort arbitrarily among the remaining devices. The optimal strategy for the inspectee is given by Theorem 7 (since U is empty), and requires always cheating on every device, a natural conclusion since all devices are tempting.

Now suppose that $q = 1$; thus $W = N$, while T and U are empty. The results are just the limiting case $q = 1$ of those given above, except for the optimal strategies of the inspectee. He/she need not always cheat on those devices D_i with the higher penalties ($P_i > P_{k+1}$), but he/she must do so with high enough probability ($c_i \geq P_{k+1}/P_i$) to keep the inspector from diverting effort from certain inspection of these devices to more frequent inspection of the others.

Finally, suppose that $q < 1$. Thus all devices are untempting ($U = N$), while T and W are empty. The right-hand side of (2.7) and (2.8) reduces to nq ; thus Case II governs if $m/n < q < 1$ while Case I governs if $q \leq m/n$.

For $m/n < q < 1$, (4.2) yields $k = [m/q]$, while (4.3) gives $g = m - q|G|$. Again the value of the game F° is given by (4.5), yielding

$$\begin{aligned} F^\circ &= V(E \cup L) - P_{k+1}g \\ &= q[P(N) - \{P(G) - P_{k+1}|G|\}] - mP_{k+1}. \end{aligned} \tag{5.2}$$

For each integer k , with $1 \leq k \leq n-1$, F° is linear in q and m (increasing with q , decreasing with m) in the angular sector $\{(m, q): k < m/q < k+1\}$ of the positive quadrant of the (m, q) -plane.

Still under the assumption that $m/n < q < 1$, the optimal strategies for the inspector are given again by (b) of Theorem 5; again the devices with penalties P_i exceeding the critical level P_{k+1} are always to be inspected, while those with lower penalties should be left uninspected. The balance (if any) of inspection resources can be allocated arbitrarily among the remaining devices, D_i , subject only to the no-overkill proviso $p_i^\circ \leq q_i$. If either G is empty (i.e., $P_{k+1} = \max_i P_i$) or if $g=0$, then the unique optimal strategy for the inspectee is given by Theorem 7: cheat on the high-penalty devices ($P_i > P_{k+1}$) with probability P_{k+1}/P_i , and always cheat on the other devices. But if $g=0$ and G is non-empty (i.e., there are m/q high-penalty devices), then Theorem 8 shows that the inspectee has an additional one-parameter family of optimal strategies specified by the behavior $P_i c_i^\circ - P_{k+1} = M(\mathbf{c}^\circ)$ on the high-penalty devices D_i (and always cheating on the other devices), where the range of the parameter $M(\mathbf{c}^\circ)$ is given by (4.11).

The only remaining situations are those with $q \leq m/n$. As noted above, Case I applies. The game-value F° is 0, by (i) of Theorem 1, so that the inspection-system succeeds in preventing illicit gains by the inspectee. In fact, if $q < m/n$ then Theorem 3 shows that the system succeeds in inhibiting all cheating (in optimal behavior) by the inspectee. If $q = m/n$, however, the inspectee has (by Theorem 4) optimal strategies involving cheating on the various devices D_i with probabilities inversely proportional to the associated penalties P_i . By Theorem 2, the optimal strategies for the inspector are precisely those in which each device is inspected with probability at least q .

6. References

- [1] Hoffman, K., Joel, L. S., and Pearl, M. H., Resource Requirements and Allocation in IRS' Audit Division, Nat. Bur. Stand. (U.S.) NBSIR 77-177, (1969).
- [2] Goldman, A. J., and Pearl, M. H., The dependence of inspection-system performance on levels of penalties and inspection resources, J. Res. Nat. Bur. Stand. (U.S.), **80B** (Math. Sci.), No. 2, 189-236 (Apr.-June 1976).
- [3] Goldman, A. J., and Shier, D. R., Player Aggregation in Noncooperative Games, J. Res. Nat. Bur. Stand. (U.S.), **85**, No. 5, 391-396 (Sept.-Oct. 1980).